ANALYSIS OF SPERM MOLECULES NEEDED FOR FERTILIZATION IN *C.ELEGANS*

by

JULIE S. HANG

A thesis submitted to the

Graduate School-New Brunswick

Rutgers, The State University of New Jersey

and

The Graduate School of Biomedical Sciences

University of Medicine and Dentistry of New Jersey

in partial fulfillment of the requirements

for the degree of

Master of Science

Graduate Program in Cell and Developmental Biology

written under the direction of

Dr. Andrew W. Singson

and approved by

_____

_____

_____

_____

New Brunswick, New Jersey

May 2009

ABSTRACT OF THE THESIS

Analysis of sperm molecules needed for fertilization in *C. elegans*

By JULIE S. HANG

Thesis Director:
Dr. Andrew W. Singson

Fertilization is the biological process through which life is propagated and genetic variation is generated. Its importance to sexually reproducing species is unrivaled, but we are far from obtaining a complete understanding of how this process occurs. This thesis is a study of sperm molecules involved in *Caenorhabditis elegans* fertilization with the ultimate goal of elucidating and understanding the function of fertilization molecules across species.

The first chapter provides an introduction to the field of fertilization, a brief overview of what is currently known, and it concludes with the use and advantages of using *C. elegans* as a model system to study fertilization.

The second chapter describes a method that utilizes single nucleotide polymorphisms (SNPs) to streamline the initial genetic mapping of newly isolated mutants. An example of this method for linkage mapping is provided, and I compare and contrast this method to traditional and other SNP approaches.

The third chapter describes the phenotypic characterization and initial mapping of the *as28* mutation resulting in a temperature sensitive sterility in *C. elegans*. The mutation causes a sperm activation defect causing abnormal spermatid morphology. Mapping of this mutant strain revealed that the observed phenotype is the result of two mutations, which has complicated characterization of this mutant phenotype.

The fourth chapter describes the cloning of *spe-13*. Mutations in *spe-13* result in worms that produce morphologically and physiologically normal spermatids that mature into spermatozoa that are unable to fertilize oocytes. The identification of *spe-13* has proved to be difficult with traditional mapping techniques due to its chromosomal position. Using whole genome sequencing, we identified *spe-13* candidate genes in an effort to clone this elusive gene.

In the final chapter, I summarize and discuss future directions for each project that has been described in this thesis work.

ACKNOWLEDGEMENTS

There are no words to describe how deeply I appreciate the support of my family and friends throughout my graduate career. There are numerous people whom I would like to thank. If they are not included in this section, it does not mean that the help I have received from them means any less to me, it just means that I am human and forgetful.

I owe everything to my parents and my brother, who have always been there for me through everything big and small. Their love and support means the world to me, and I would be lost without them.

I am grateful to have such great friends who have stuck by me and kept me sane. A special thanks to Forum, Vanessa, Sherry, Karen, John, Riza, Patty, Julia, Eric, and Ryan; and Mike, a recent addition to my life, but whose presence has made a huge difference in the last couple of months.

I would also like to thank my advisor, Andy, for his optimism, knowledge, and mentoring. He has shown me the importance of balancing science with other pursuits in life. Thanks to my committee members, Drs. Chi-hua C. Groff, Monica Driscoll, Barth Grant, and Kim McKim for their advice and insight on my projects.

My lab mates Pavan, Rika, and Indrani, who have helped me troubleshoot the little bumps and quirks I have encountered in my experiments, I owe them more than a thank you. Thanks to Betty, Stephanie, Julianna, Jean, Marty, Jon, and Ariel who made lab life enjoyable and memorable.

Finally, I would like to thank all the people working in the various offices that have helped me during my time at Rutgers.

TABLE OF CONTENTS

LIST OF TABLES

LIST OF ILLUSTRATIONS

CHAPTER 1

An introduction and overview of molecules involved in fertilization and the use of *Caenorhabditis elegans* as a model system

Introduction:

For many species, sexual reproduction is the only way through which genetic information is passed from generation to generation. The union of two haploid gametes at fertilization is the means by which sexual reproduction occurs. Fertilization research has been conducted in many invertebrate and vertebrate systems, such as sea urchin and mouse. These studies have led to the discovery and identification of several molecules involved in oocyte recognition by sperm, sperm-oocyte adhesion and membrane fusion, and egg activation [2-9].

Oocyte recognition by sperm

Mammalian sperm, upon reaching the female reproductive tract, undergo a process called capacitation, which results in the loss of membrane components and hyperactive movement [10, 11]. Capacitation is required for sperm to penetrate the cumulus cells and zona pellucida to reach and fuse with the oocyte plasma membrane during fertilization.

Sperm have to travel long distances to reach the oocyte, and this process is thought to be facilitated by a chemical attractant released by the oocyte [12] such as asterosap in starfish and resact in sea urchins [13-16]. These peptides initiate a cyclic guanosine monophospate (cGMP) signaling cascade in sperm hypothesized to result in sperm chemotaxis [17].

Once the sperm locates and reaches the oocyte, there are several barriers it must overcome to reach the oocyte plasma membrane. The mammalian oocyte is surrounded by a layer of cumulus cells; sperm must navigate and digest their way through the extracellular matrix of these cells [5]. After the cumulus cells, sperm encounter the zona pellucida (ZP), the oocyte extracellular matrix that is made of 3 major glycoproteins: ZP1, ZP2, and ZP3 [5]. The sperm, upon binding to the zona, undergoes the acrosome reaction, releasing the enzymes needed to penetrate the zona pellucida [5, 18]. It is hypothesized that sperm interact with the zona pellucida via ZP3 due to the

inhibition of sperm-zona binding when sperm is pre-incubated with ZP3 [19]. This hypothesis has yet to be substantiated due to the lack of zona formation in ZP3 null mice and species-specific glycosylation [5]. Finally, the sperm enters the perivitelline space, where it encounters the oocyte plasma membrane to initiate fusion [5, 18].

Molecules that facilitate sperm-oocyte fusion

The molecular mechanism by which sperm-oocyte fusion occurs remains unknown. This is not to say that this process is not well studied or understood. A number of molecules present on the sperm or oocyte plasma membrane have been shown to be involved in the fusion process: fertilin αβ, cyritestin, and Izumo on the sperm plasma membrane and CD9, integrins, and glycosylphosphatidylinositol (GPI)-anchored proteins on the oocyte plasma membrane. Of these proteins, only Izumo and CD9 are known to be directly required for fusion to occur. This section seeks to provide an overview of the molecules known to be involved sperm-oocyte fusion.

In mammals, two members of the ADAM (a disintegrin and metalloprotease) integrin membrane protein family, fertilin α and fertilin β (also known as ADAM-1 and ADAM-2), are known to mediate sperm-oocyte fusion. Fertilin α and fertilin β dimerize on the sperm surface and were identified as a result of mono-clonal antibody inhibition of sperm-oocyte fusion [20]. Sperm isolated from mice lacking fertilin β have defects with sperm entry into the oviduct, cannot bind to the zona pellucida, and have a decreased ability to fuse with the oocyte plasma membrane [21]. These observations suggest that fertilin β is involved in sperm-oocyte membrane interactions, perhaps fusion, and it may have roles in binding of sperm to the zona pellucida and/or migration of sperm in the oviduct. A putative fertilin β receptor on the oocyte membrane is the α6β1 integrin [22-24], however oocytes that lack the α6 integrin are still capable of being fertilized [25].

Another member of the ADAM family, cyritestin (ADAM-3), is expressed solely in the mouse testis. Synthetic competitor peptides derived from the disintegrin domain of cyritestin [26, 27] were found to inhibit *in vitro* fertilization. Isolated cyritestin domains [24] and antibodies to cyritestin [27] inhibited sperm-oocyte fusion. Sperm lacking cyritestin, like those that lack fertilin β, are unable to adhere to the zonae pellucidae [28]. But unlike sperm lacking fertilin β, the lack of cyritestin does not affect the ability of these sperm to fuse with zona-free oocytes [28]. Cyritestin is hypothesized to act during the interaction between the sperm and the oocyte zona pellucida.

Izumo, a member of the immunoglobulin superfamily, has been found to be directly involved in sperm-oocyte membrane fusion. It is the first and as of yet, the only sperm membrane protein identified that is essential for fusion. The protein localizes to the sperm surface only after the acrosome reaction [11]. Sperm derived from males lacking Izumo are able to migrate through the oviduct, and to bind and penetrate the zona pellucida [29]. These sperm bind to the plasma membrane of zona-free oocytes, but are unable to fuse with them [29]. Oocytes injected with Izumo deficient sperm become fertilized and are able to undergo activation and successful implantation [29], suggesting that Izumo function is required for sperm-oocyte fusion.

A possible partner for Izumo is CD9, a tetraspanin on the oocyte plasma membrane. Oocytes lacking CD9 cannot be fertilized by wild-type sperm; sperm found in the perivitelline space (PVS) of these oocytes were unable to bind the oocyte plasma membrane and moved about actively [30, 31]. Along with being distributed on the oocyte plasma membrane, CD9 has been observed to be present in vesicles found in the PVS [32]. CD9 containing vesicles from unfertilized wild-type oocytes have been shown to mediate sperm-oocyte fusion between sperm and mutant oocytes lacking CD9 [32]. This observation suggests that the sperm-oocyte fusion process begins before direct cell membrane interactions.

An association between CD9 and the α6β1 integrin has been shown [33], suggesting that CD9 may be involved in regulating other oocyte membrane molecules. This association provides support for the "tetraspanin web" hypothesis [34], proposing that a network of interactions resulting from the ability of tetraspanins to interact with themselves and with other proteins, on the oocyte plasma membrane. The molecular function of CD9 has yet to be determined and appears to be a complicated story. It may be directly involved in sperm-oocyte fusion, it may facilitate fusion that is directed by other molecules, it may regulate a protein or proteins involved in fusion via the "tetraspanin web", or it may perform all these functions along with others not yet detected.

Integrins and GPI-anchored proteins on the oocyte plasma membrane are also thought to be involved in sperm-oocyte membrane fusion. Recent studies have shown that integrins are not essential for fusion to occur. Oocytes which lack the α6β1 integrin have been shown to be fertilized *in vitro* [25]. The loss of GPI-anchored proteins in oocytes results in reduced sperm-oocyte binding and fusion [35]. GPI-anchored proteins are enriched in lipid rafts, microdomains on the plasma membrane, and the loss of these proteins could disrupt these domains, resulting in defective fusion [11].

The components identified to act at sperm-oocyte fusion have been studied in great detail, but there are components in this pathway that are yet to be identified and characterized. One way to identify such molecules would be to identify the proteins which interact with CD9 directly or indirectly through the tetranspanin microdomain. Another avenue would be to elucidate molecules on the oocyte membrane which interact with Izumo. Identifying additional components will aid in uncovering the underlying mechanism of sperm-oocyte membrane fusion. It will also be interesting, and perhaps informative, to see if the factors involved in sperm-oocyte fusion are conserved across species.

Egg activation

After the sperm and oocyte have joined together, the fertilized egg undergoes egg activation. During egg activation, the egg completes meiosis, the male and female pronuclei fuse, a block to polyspermy is established, and embryonic development is initiated. This process is thought to be induced by an increase in calcium (Ca^{2+}) concentration and a Ca^{2+} wave resulting from sperm-oocyte fusion [36].

Calcium-dependent egg activation has been shown to be conserved across animals [36]. There exists a difference between protostomes and deuterostomes in how the increase in Ca^{2+} is achieved: protostome eggs generate an increase in Ca^{2+} by an external influx of Ca^{2+}, whereas deuterostome eggs release intracellular Ca^{2+} from the endoplasmic reticulum (ER) [37]. Calcium is released from the ER via the inositol 1,4,5-trisphosphate receptor (IP_3R) at fertilization; this mechanism is conserved among all species that experience an intracellular Ca^{2+} increase [38]. As a result of the change in intracellular Ca^{2+} concentration, the cortical granule reaction is activated. The enzymes released by the cortical granules alter the zona pellucida glycoproteins, which is thought to establish the block to polyspermy to prevent penetration by other sperm [39].

Due to the timing of the Ca^{2+} increase in eggs after fertilization, it has been hypothesized that a sperm factor is involved in initiating this increase. There are two proposals on how this is achieved. The first model involves a sperm ligand on the oocyte plasma membrane which initiates a signaling cascade resulting in activation of phospholipase C (PLC) and the hydrolysis of phosphatidylinositol 4,5-bisphosphate (PIP_2) to inositol 1,4,5-trisphosphate (IP_3) [3]. The other model proposes that there is a soluble sperm factor which is released into the egg cytoplasm after fusion; this model is dubbed the sperm factor hypothesis [36, 39, 40]. It has been observed that

injection of sperm cytoplasmic extracts into oocytes triggers Ca^{2+} activity similar to those observed during fertilization [41-44].

Studies in sea urchin egg homogenates suggested that the sperm factor responsible for the release of Ca^{2+} is a PLC present in sperm extracts [45, 46]. PLCξ (phosolipase C zeta) is a novel PLC identified to be only expressed in mammalian spermatids [47]. Injections of PLCξ cDNA into oocytes lead to Ca^{2+} oscillations similar to those observed in fertilization [47, 48], supporting its role in stimulating Ca^{2+} release. There appears to be variations in amounts [49] and potency [50] of PLCξ from species to species, suggesting that the amount and potency of PLCξ is specific to each species and is maximized by each species to induce egg activation in corresponding oocytes [40].

The localization and regulation patterns of PLCξ in both the sperm and the egg remain unknown. PLCξ is very sensitive to Ca^{2+} [40], and it is perplexing how PLCξ is retained for long periods of time in mature sperm which have a Ca^{2+} concentration similar to that of eggs [51]. Since PLCξ was discovered in mammalian spermatids, it would be interesting to see if there are homologous or analogous factors in other species which may aid in understanding its localization and regulation patterns.

Use of *Caenorhabditis elegans* for studying fertilization

C. elegans serves as an excellent model system to study fertilization. Advantages of *C. elegans* include a short life cycle (3.5 days when grown on *Escherichia coli* at 20°C) [52], the ability to generate a large number of progeny (250-300 self progeny per wild type hermaphrodite) for large scale genetic analysis, and a transparent cuticle for direct visualization of *in vivo* fertilization-associated events under the light microscope. The genome of *C. elegans* is fully sequenced,

allowing for the use of both forward and reverse genetic approaches to study the genes involved in fertilization.

There are two sexes in *C. elegans*: hermaphrodites and males. Both hermaphrodite and male worms start sperm production during the last larval stage (L4), but hermaphrodites stop sperm production and switch to oocyte production upon maturation to adulthood. Sperm in the hermaphrodite is stored within the spermatheca, also the site of fertilization [53] (Figure 1.1).

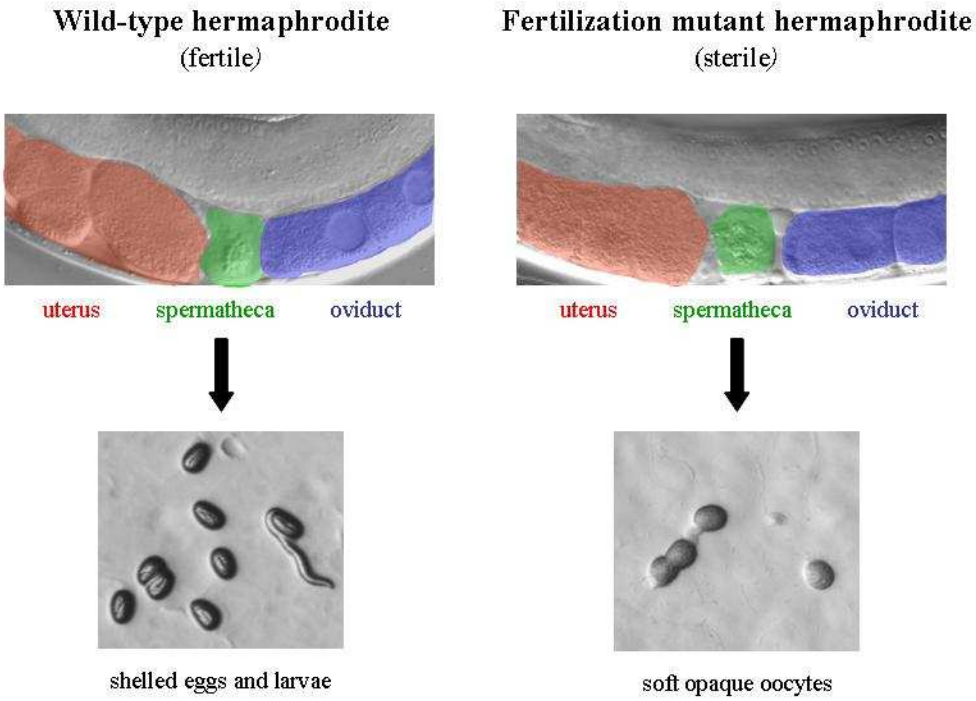

Figure 1.1: *C. elegans* reproductive tract and fertilization mutant phenotype. The reproductive tract is comprised of the oviduct (blue), spermatheca (green), and uterus (red). In wild-type hermaphrodites, fertilized embryos are present in the uterus, which are laid on to culture plates as shelled eggs which hatch into larvae. In fertilization mutants (Spe, Fer, or Egg), the uterus is filled with unfertilized oocytes, which are laid on to the culture plate as spongy round oocytes.

C. elegans sperm characteristics

C. elegans sperm differs from mammalian sperm by being amoeboid with a pseudopod and lacking an acrosome and flagellum. Despite these differences, they still carry out the same fundamental functions associated with all sperm. Sperm, irrespective of size or shape, must be able to acquire motility, locate and move toward an oocyte, bind to the oocyte, fuse with, or enter

the oocyte, provide paternal information, and ultimately, activate zygotic development. Due to the universal nature of sperm function and the relative simplicity and accessibility of its reproductive system, *C. elegans* provides a good model system to study sperm development and action at fertilization.

C. elegans sperm undergo activation (spermiogenesis) in which round sessile spermatids are transformed into motile spermatozoan with pseudopods [4, 54]. Sperm activation is necessary for the attainment of sperm motility and localization to the spermatheca. Hermaphrodite-derived sperm are activated during the first ovulation event, whereas male-derived sperm are activated by male seminal fluid [54]. During activation, Golgi-derived organelles called membranous organelles (MOs) localize to and fuse with the plasma membrane. This fusion results in the distribution of MO contents on the sperm plasma membrane [55]. Sperm are unable to fertilize oocytes if MO fusion does not occur and its contents are not properly distributed on the plasma membrane.

A characteristic of *C. elegans* sperm is that male-derived sperm can out-compete hermaphrodite-derived sperm. When hermaphrodites are crossed to males, a large percent of the oocytes are fertilized by male sperm [53, 56]. Mutant males with defects in sperm function are still able to out-compete and suppress hermaphrodite-derived sperm though they are unable to fertilize oocytes [57].

When everything proceeds normally in *C. elegans*, an oocyte is fertilized upon entry into the spermatheca by a single sperm [58]. The fertilized egg is then pushed out of the spermatheca into the uterus and eventually laid through the vulval opening. During this process, sperm are pushed out of the spermatheca by fertilized eggs passing into the uterus; these sperm must re-localize to the spermatheca in order to fertilize the next oocyte [53].

The nature of the reproductive biology of *C. elegans* makes it a good model for the genetic analysis of *spe*rmatogenesis defective (*spe*), *fer*tilization defective (*fer*) or *egg* defective (*egg*) mutants, all of which present with a sterile phenotype (Figure 1.1). Spermatogenesis (Spe) mutants are self-sterile; mutant hermaphrodites cannot self-fertilize and are unable to produce self progeny due to a sperm defect. These sterile mutants, upon mating to wild-type (N2) male worms, are capable of producing outcross heterozygous progeny (Figure 1.2). The sterile phenotype of Egg mutant phenotypes cannot be rescued by crossing to wild-type males due to defects in their oocytes. This distinction allows for the rapid separation of Spe and Egg mutants from screens for fertilization defective mutations.

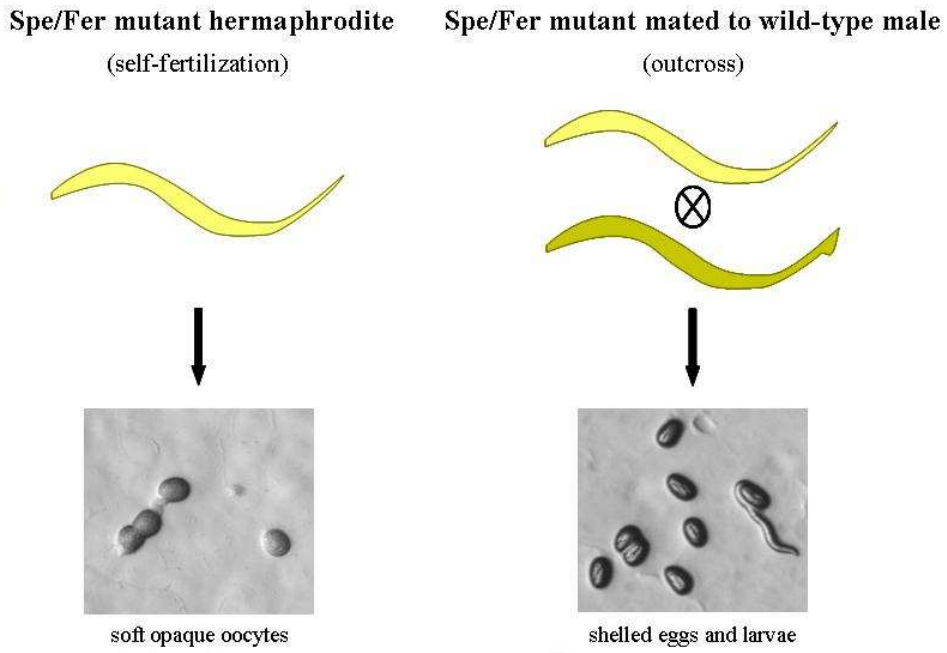

Figure 1.2: Rescue of Spe or Fer mutant hermaphrodites by outcrossing to wild-type males. Spe or Fer mutant hermaphrodites are self-sterile and do not produce progeny. When these Spe or Fer mutant hermaphrodites are crossed to wild-type males, they are able to produce viable outcross progeny.

C. elegans sperm molecules that function at fertilization

Some sperm genes involved in fertilization include *spe-9, spe-13, spe-36, spe-38, spe-41/trp-3, spe-42,* and *fer-14.* Brood counts of these mutant hermaphrodites showed these mutants have decreased brood sizes when compared to wild type, but have normal ovulation rates. Worms with mutations in these genes have normal mating behaviors and mutant males are able to successfully transfer their sperm to hermaphrodites after copulation. Sperm derived from mutant males of this class are able to localize correctly to the spermatheca and make contact with oocytes, but are unable to enter and fertilize them, supporting the conclusion that these sperm genes are required for fertilization. Sperm isolated from mutant males and hermaphrodites have wild-type morphology and activation (Figure 1.4), suggesting that the defect is in sperm function and not in sperm development or activation. Electron microscopy showed that hermaphrodite-derived mutant sperm of these genes are not missing key organelles and are morphologically indistinguishable from wild-type sperm. The cloning and characterization of *spe-9, spe-38,* and *spe-41/trp-3* have uncovered a small part of the molecular mechanism driving the fertilization pathway; *spe-13, spe-36,* and *fer-14* remain yet to be cloned.

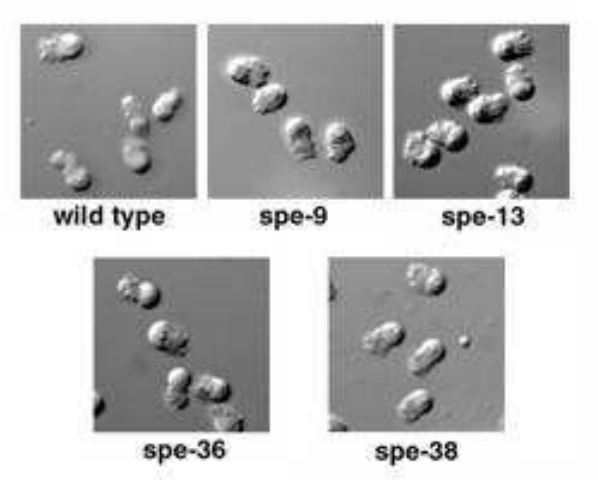

Figure 1.4: Spe mutant sperm morphology. Sperm derived from sperm function mutant males have normal morphology and activation that is indistinguishable from sperm derived from wild-type males.

The first cloned and characterized sperm gene that functions at fertilization is *spe-9* [59, 60]. The *spe-9* gene is predicted to encode a single-pass transmembrane molecule with 10 epidermal growth factor (EGF) domains in its extracellular region [60]. SPE-9 has a dynamic localization pattern: SPE-9 is found on the sperm plasma membrane of unactivated spermatids, and after activation, it is found on the pseudopod [61]. Mutations in the EGF repeats result in varied effects on fertilization [62]. Some repeats seem more dispensable than others, resulting in defects under restrictive temperature conditions, and others which eliminate SPE-9 function completely when altered [62]. However, SPE-9 molecules which do not contain the transmembrane domain are non-functional and the removal of the cytoplasmic tail does not seem to affect its function [62]. SPE-9 is hypothesized to be one half of a ligand-receptor pair due to the presence of EGF repeats in many ligand-receptor molecules [63], and its localization on the sperm pseudopod, which is hypothesized to be the region which contacts the oocyte during fertilization [61]. Sperm genes with the same mutant phenotype as *spe-9* are often referred to as “sperm function mutants”.

spe-38 was identified as a gene on chromosome I, and is predicted to encode a protein with four-pass integral membrane domains [64]. SPE-38 localizes to the membranous organelles (MOs) in spermatids and moves to the pseudopod during sperm activation [64]. There are no apparent homologs to SPE-38 outside of nematodes.

Localization of SPE-38 in other fertilization mutants and of sperm molecules in *spe-38* mutants was determined via immunostaining to determine if SPE-38 localization is influenced by other molecules or if SPE-38 affects localization of other molecules. These experiments showed that SPE-38 does not localize to the pseudopod in *fer-1* mutants, in which MO fusion does not occur, and that SPE-41/TRP-3 movement during spermiogenesis is hindered in *spe-38* mutants

(Chatterjee, personal communication). An interaction between SPE-38 and SPE-41/TRP-3 is hypothesized to occur due to this dependence in localization patterns.

SPE-41/TRP-3 belongs to the transient receptor potential (TRP) family of cation channels. It has been implicated in sperm-oocyte interactions during fertilization [65]. In spermatids, SPE-41/TRP-3 localizes to the MOs and upon activation translocates to the plasma membrane, and the loss of TRP-3 in *C. elegans* sperm is correlated with a defect in calcium influx [65]. Calcium influx in mammals is associated with cell-cell fusion. Members of the TRP family are also expressed in mouse sperm, further suggesting that TRP proteins are involved in sperm-oocyte interaction and fusion.

Mutations in *spe-42* phenocopy other sperm function mutant phenotypes. SPE-42 is predicted to encode a 7-pass integral membrane protein with a cytoplasmic N-terminal and an extracellular C-terminal [66]. Localization of other genes belonging to the *spe-9* class (SPE-9, SPE-38, SPE-41/TRP-3) is unaffected in *spe-42* mutant sperm [66]. There are SPE-42 homologs in many species including worms, mice, and humans; although these homologs are also predicted to be multi-pass membrane proteins, they do vary in the number of the transmembrane domains. The presence of SPE-42 homologs across many species suggests that this function of this molecule may be conserved and that these homologs may play a role in fertilization in their respective species.

So far studies of fertilization in *C. elegans* have been focused on elucidating and characterizing sperm molecules. Since fertilization requires the meeting of two components, the sperm and the oocyte, recent studies have shifted some of the focus towards molecules found in or on the oocyte that affect fertilization.

Egg molecules in *C. elegans* that affect fertilization

Genes that regulate or are directly involved in oocyte function are frequently discovered via RNAi screens. Two examples are EGG-1 and EGG-2, both of which encode type II transmembrane molecules containing LDL receptor. Hermaphrodites with loss of function mutations or EGG-1 or EGG-2 RNAi treated hermaphrodites have decreased fertility; mutations or RNAi knockdown in both EGG-1 and EGG-2 results in complete sterility [67]. This observation suggests these two proteins play semi-redundant roles are a likely the result of a gene duplication event. Male worms that lack EGG-1 or EGG-2 have wild-type fertility levels and sperm production and morphology. Immunofluorescence and green fluorescent protein (GFP) constructs of EGG-1 show the protein to be localized at the oocyte plasma membrane [67]. Ovulation rates in *egg-1* mutants are lower than those of wild-type, and sperm from the spermatheca of these mutants are lost at a rate faster than wild-type. The current model is that EGG-1 and EGG-2 are receptors which bind to sperm ligands during fertilization.

Another oocyte molecule, EGG-3, does not function directly at, but indirectly affects fertilization. Hermaphrodites that lack EGG-3 as a result of knockdown by RNAi are sterile, whereas males retain their fertility [68]. It was shown that *egg-3* mutant oocytes are capable of being fertilized by sperm, but egg activation after fertilization is defective [68]. EGG-3 belongs to the protein tyrosine phosphatase like (PTPL) family. Members of this family lack the critical catalytic residues found in protein tyrosine phosophatase and are thought to regulate phosophatase activity by sequestering or competing for target molecules. EGG-3 is hypothesized to be a part of a protein complex that is needed for the detection of sperm entry and egg activation [68].

EGG-4 and EGG-5 are also members of the PTPL family that result in hermaphrodite sterility when mutated or knocked down; these proteins are predicted to be 99.2% identical with redundant functions. Hermaphrodites treated with *egg-4/5* RNAi exhibited defects in egg

activation after fertilization including eggshell formation, polarized cytoskeletal rearrangement, and polar body formation and other meiotic defects (Parry, personal communication). In developing oocytes, EGG-4/5 is found on the plasma membrane and becomes cytoplasmic in embryos. This dynamic localization pattern is dependent on EGG-3 and CHS-1, a chitin synthase required for eggshell formation. Conversely, EGG-4/5 is needed for the proper re-distribution of EGG-3 and CHS-1 after fertilization (Parry, personal communication). The current model proposes that EGG-3, EGG-4, and EGG-5 act as anchors to sequester molecules which release them at the proper time during egg activation.

The importance of successful fertilization to sexual reproducing species is unrivaled; optimization of this process allows the events to occur smoothly and the propagation of genetic material, in essence life, to the next generation. Infertility is a common issue many people face today, resulting in an entire industry based on assisted and *in vitro* reproduction. Gaining a better understanding of the underlying molecular mechanism of fertilization may enable us to uncover the root causes of infertility in order to develop treatments or alternative methods. On the other hand, information gathered from studies of fertilization molecules may be used to generate novel contraceptive strategies designed at the molecular level. The benefits and knowledge gained from studying fertilization can solve fertility issues in other species. There are a number of endangered species that have difficulty reproducing in captivity. Also, contraceptive methods could be designed to control the overpopulation of certain animals, such as deer, in densely populated areas.

The information obtained from studying the molecular mechanism of fertilization does not only enrich the understanding of the field of reproductive biology. The interactions between sperm and oocyte have many similarities to signaling systems used in somatic cells [8, 69]. In addition, cell-cell and membrane fusion events that are involved in many essential cellular processes, such as

vesicular transport [70], and the fusion of sperm and oocyte during fertilization may be analogous. Molecules involved in sperm-oocyte fusion may have counterparts in other cellular fusions, making it easier to identify, study, and understand such molecules and their respective biological processes.

CHAPTER 2

Use of single nucleotide polymorphisms to facilitate gene mapping in *Caenorhabditis elegans*

Introduction:

A common goal in biological studies is to understand the molecular mechanisms involved in driving biological processes. To achieve this goal, the molecules involved in these processes and pathways need to be identified and their functions elucidated. One way to identify molecules is through forward genetic screens, in which phenotypes of interest are generated and the genomic position of the mutations are determined through gene mapping and cloning techniques. Depending on a gene's physical location, the time it takes to clone it can range from months to years; there are genes that have been characterized but remain uncloned. Simple, efficient, and accurate mapping techniques could greatly reduce the amount of time spent identifying and cloning genes, allowing for more time and resources to be focused on determining their molecular function and role in biological pathways.

Single nucleotide polymorphisms (SNPs) have emerged as a powerful tool for fine-tuned mapping and cloning of genes across model systems [71-74]. SNP mapping technique is similar to that of traditional mapping techniques to link a mutation to a chromosome, and two-factor and three-factor mapping to map out borders for the region in which the mutation is located.

SNP mapping has several advantages over mapping with visible phenotypic markers: 1) SNPs do not have visible phenotypes so they cannot be masked or altered by other phenotypes; 2) the density of SNPs across genomes is higher than the density of visible markers; 3) the presence or absence of SNPs can be easily detected and verified with standard molecular biology techniques. Whole-genome sequencing for mutant allele identification [75] coupled with initial linkage and interval mapping with SNPs can greatly reduce the amount of time and effort needed to clone genes [75, 76].

Traditional SNP mapping involves the polymerase chain reaction (PCR) amplification of the region containing the polymorphism and sequencing of that region for detecting the presence of the SNP. This procedure allows for the use of all the SNPs present in a genome, but it is labor intensive and can be expensive. Strategies have been developed in which the PCR product is analyzed directly with fluorescently tagged probes [77] or through denaturing high-performance liquid chromatography (DHPLC) [78, 79]. Although these strategies are more efficient, they can also be costly and labor intensive. A different approach utilizes SNPs that introduce insertions or deletions (indels) or snipSNPs. Indels are easily identified by running the PCR product directly on agarose gels, but they may require visualization on high-resolution agarose gels or involve large regions that are inserted or deleted in the DNA sequence. snipSNPs, SNPs that result in restriction fragment length polymophism (RFLPs) between different strains, the most commonly used lab strains being Bristol N2 and Hawaiian CB4856, are easier to verify than sequence SNPs. The nature of snipSNPs allow for easy visual detection of the presence or absence of that SNP through a simple restriction digest assay of the PCR product at a relatively low cost. The advantages of using snipSNPs in mapping have resulted in its wide use and popularity.

The use of SNPs is an easy and efficient way to determine genetic linkage to *C. elegans* [80] chromosomes. Strategies have been developed that involve more in-depth primer sets for high-throughput gene mapping [81-83] to streamline the mapping process to allow for rapid and precise interval mapping. These strategies [81-83] offer many advantages which include: generation of bulk lysates for analysis, ability to use one lysate for multiple SNP analyses, and optimized primer sets for identical amplification conditions. However, a disadvantage of these published sets is that some of the included snip-SNPs result in the digestion of both N2 and CB4856 sequences at differing positions, making the agarose gels difficult to interpret.

The method described here provides a wide-ranging list of primer sets for 41 snip-SNPs that generate restriction sites only in CB4856 but not N2. Selecting SNPs that digest sequence only from one strain allows for precise and unambiguous agarose gel banding patterns that determine the presence or absence of CB4856 sequence. This procedure was designed for smaller-scale gene mapping and for unambiguous SNP detection. The snipSNPs are spread out over all chromosomes (7 per autosome, and 6 for the X chromosome), allowing for linkage assignment and interval mapping. The purpose of developing this primer set was not to compete with previously published works, but rather to serve as a potential alternative.

Whole-genome sequencing has been shown to be a viable option for rapid gene cloning in *C. elegans* [75]. This technique when combined with rapid linkage and interval mapping with SNP markers can be a powerful tool in the cloning and identification of new genes.

Methods:

Culturing of *C. elegans* strains

Culturing of *C. elegans* was done according to standard protocols described elsewhere [52]. The strains used in this work were: *dpy-5(e61)*, *rol-1(e91)*, *unc-32(e189)*, *as28*, Bristol strain N2 (wild-type), and Hawaiian strain CB4856. Strains were obtained from the *Caenorhabditis* Genetics Center (CGC, University of Minnesota). The *as28* mutation was isolated in an ethyl methanesulfonate (EMS) mutagenesis screen conducted by Indrani Chatterjee and Emily Putiri. All strains were Bristol-derived except for the Hawaiian strain.

Genetic crosses

Adult mutant hermaphrodites (*dpy-5;rol-1;unc-32* and *as28)* were mated to Hawaiian males at a ratio of 3 males to 1 hermaphrodite. F1 heterozygotes were allowed to self-fertilize, and 60 to 75 homozygous mutant F2 animals were selected based on phenotypes (Figure 2.1).

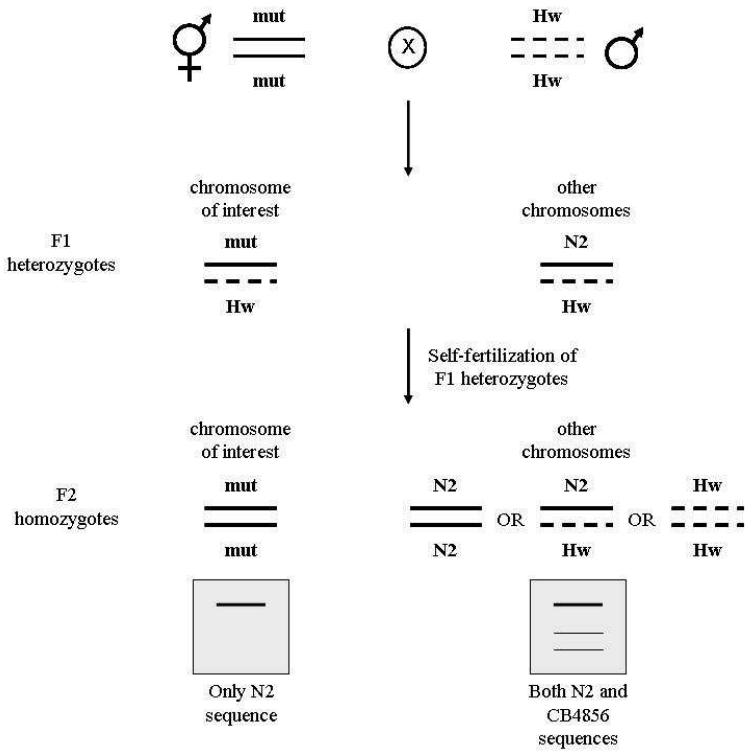

Figure 2.1: Schematic of genetic cross to CB4856. The boxed regions depict hypothetical banding pattern on an agarose gel for the SNPs listed in this work.

DNA extraction

Adult worms were selected based on mutant phenotype and grown together on a culture plate overnight. The worms were then washed with 1X M9 buffer solution and collected into tubes containing 60 µl worm lysis buffer (50 mM KCl, 10 mM Tris-HCl pH 8.3, 2.5 mM $MgCl_2$, 0.45% NP-40, 0.45% Tween 20, 0.01% gelatin, 60 µg/ml Proteinase K). The worms were lysed by incubating at 65°C for 60 minutes, followed incubation at 95°C for 15 minutes. Worm lysates were generated for Bristol (N2), Hawaiian (CB4856), the original mutant strain (*dpy-5;rol-1;unc-32* or *as28*), and homozygous mutant F2 animals (*dpy-5;* CB4856 or *as28;* CB4856) from the cross described above.

SNP selection

SNP information on CB4856 from the publicly available SNP information site (http://genome.wustl.edu/genome/celegans/celegans_snp.cgi) was used to select SNPs that would

result in RFLPs in CB4856, but without affecting the N2 sequence. SNP restriction digest patterns were verified with N2 and CB4856 PCR products. The SNPs developed and used in this work are listed in Table 2.1.

PCR and restriction digest

PCR was carried out on 2.5 µl of each worm lysate by adding each lysate to 22.5 µl of a PCR master mix (0.25 µl 25 µM forward primer (listed in Table 2.1), 0.25 µl 25 µM reverse primer (listed in Table 2.1), 22.0 µl sterile ddH_2O in a tube containing one PCR bead (GE #27-9559-01). The reactions were subjected to the following cycling conditions: 94°C 120s; 30 cycles of 94°C 30s, 58°C 60s, 72°C 60s; 72°C 420s. Restriction digest of each PCR was done by adding 10µl of each PCR to a master digest mix (2 µl 10X buffer, 1 µl restriction enzyme (listed in Table 2.1), and 7 µl sterile ddH_2O). Digests were incubated at 37°C for at least 1 hour. Digested samples (20 µl digest reaction) were loaded onto a 1% agarose gel for visualization.

Table 2.1: List of location, primer sequence, restriction enzyme, PCR and digest size for each SNP. For each primer pair, the forward primer is listed first in a 5' to 3' direction. Genetic positions are from Wormbase [1], release WS196. *denotes chromosomal linkage SNPs, †denotes CB4856 PCR size

Linkage Group	Genetic Position	Clone	Primer Sequences	PCR (bp)	Enzyme	CB4856 Digest (bp)
I	-19	F53G12	GTGGACGAGATTTTGTGGCTGG GCCCACCCCCACCCAAT	890	EarI	309, 312, 578, 581
I	-8	F32B5	CCGCTATCTCCGCTGACCCG TCGTATCCGCTGAGGTGAAG	1058	MboII	487, 488, 571, 572
I	0	C09D4	ATCTCCAATCACTAGCGACGACT TGCGAAGAAACTGATTGTCCTGG	1139	AvaI	556, 560, 579, 583
I	2	T23G11*	TGTATCATTTGTCCTGCTTCCCAC GACTATTCCAACAGATGTATTCAAGCCAC	811	DdeI	200, 203, 608, 611
I	3	Y67A6A	CTGGTATGCGTAGTCTGCGGG AGGTAGCTGAGTTCCAGTTTTTGC	1007	BclI	269, 273, 734, 738
I	17	Y26D4A	AGACTGTAGATTGAAAAGGGGTGTAAGAGG AGTAACAGTATGGAGAACACCAGGAAGT	821	HgaI	190, 195, 626, 631
I	28	ZK909	CACAAGTGGTTTGGAAGTACCG CAACAAAGGGATAGATCACGGG	451	HindIII	211, 215, 236, 240
II	-15	F46F5	TTTGTTCGTGATGAGATTTTCCTGG AGTTTAGCCTTTGGTGGATTCATACA	1273	XcmI	688, 689, 584, 585
II	-8	Y25C1A	GGGTCACAAGGTCACAGGTTCAA TTAGGCATAGGCTTAGGCATAGGAATAG	945	AgeI	341, 345, 600, 604
II	-1	K05F1	GTGATAAAAGTGAGTATTGATATGAGCCC GCATCACATTGGACACGAGTTATG	969	SspI	460, 509
II	0	ZK1290*	CCGTAGTTTGATTCGCAGC GGCTTTCGGACTCACGGCTT	1003	AgeI	493, 510
II	1	T24H10	ACTCTGTATTTTGATTTCTGGACTCTCGC ATAAAGTTGGTGATGACAGTGGAGCA	1018	BbsI	500, 504, 514, 518
II	6	Y57A10A	TCTGTCCATTTTCTCCCTTTGTTCC CGGTAATCCTCCATCTTCGCTTT	951	KpnI	394, 398, 552, 557
II	23	F57C2	GTAATCATCATCACGCAAATAGAAAGC CGACAACCGAATGAACTTGGG	1163	AflIII	560, 564, 599, 603
III	-26	T22F7	GACCGCCCAGGAGATGTGAAC ACTTATCACATTTTCGGTTGCCT	972	BsrI	339, 341, 631, 633
III	-10	Y71H2AM	AGGAAGTTGCCGTGTCAAATGTAA CACATCCGTAGAGCCCAATCAGA	1089	XhoI	236, 240, 849, 853
III	-4	C36A4	GCAAGAACGACAGAAAATATGGAAACA TAAGAGAAGATGTGGAGTTTTTTGAAC	896	AvaI	399, 403, 493, 497
III	-1	K04C2*	GCACAGAGAACCACCATTTGACC CTCTCAGCAAGCACAATCTGGTG	1079	HinfI	384, 387, 692, 695
III	2	M04D8	TTCGGTTGGATTTTCTATGGGTTTG TGGAATCAGAGACAGGAAAATGCC	1143	MscI	592, 551
III	11	Y41C4A	ATTCCCGCCATTTTTTTTCG ATTATTGTTGAAGAAAGGGAGGAGGATT	934	AvaII	449, 452, 482, 485
III	21	T25C8	CGGTGGTGGTAAAAGTGTAAC CAACATTCAGGCTGTGCTTTCC	544	Hpy188III	268, 270, 274, 276

Table 2.1 (Continued): List of location, primer sequence, restriction enzyme, PCR and digest size for each SNP. For each primer pair, the forward primer is listed first in a 5' to 3' direction. Genetic positions are from Wormbase [1], release WS196. *denotes chromosomal linkage SNPs, †denotes CB4856 PCR size

Linkage Group	Genetic Position	Clone	Primer Sequences	PCR (bp)	Enzyme	CB4856 Digest (bp)
IV	-26	Y66H1A	TTTCAATACGGCGTCCTG GATTCCGTCACTGGTTACTGAG	494	MboI	200, 204, 290, 294
IV	-9	T04C4	TTTGTGGCGGTTGCGTCTATTC CGATGACCGCCTCCCACG	1005	BclI	461, 465, 540, 544
IV	-3	B0212	CGTCATCAGTCACCCCGCC ACTACTTATTACACAAAACATTGGCTGAAA	1004	NspI	465, 469, 535, 538
IV	3	R05G6*	ATTCTCCCTCTCATTTTCTCATCGCT CCCATCTCATAATAACAGCATCCAAAAT	912	PstI	423, 427, 485, 489
IV	5	C08F8	GCCGACTAAGAAAGTGTCTGGAAATT CCACTGTGTCACGATTCATTGATGAT	1139/1142†	BseRI	421, 423, 719, 721
IV	12	Y64G10A	TGCCTGTGAGACTTTATGGGAAC CCACCAAGCCCAAATCAAGAAG	786	PsiI	390, 396
IV	17	C06A12	AGCGACAACTACACTTGATGGAG CGTATTTTTCGCATTGTTTCCAGG	1418	BsmFI	702, 706, 712, 716
V	-20	ZK488	CTTTTATGTCTCTTGAACTTGAATTGCTA ATCTTATTTTCAGGGCTACGC	950	BsiHKAI	459, 463, 487, 491
V	-12	F35F10	TGGCTCGGCGGAAGATTTG GCTTGCTTCTGTGGGCTTCATC	988	XmnI	450, 538
V	0	F13H6*	TCATGTCTAGTAGCCTTCGTTATTCCG AAATAGGAATGGAGTCTCGGGCTT	1104	MscI	439, 665
V	2	C50F4	GGTTTTAGACAGCGGAGGGC TTGAAACCTAAACTCACCCATTG	1004	BsmAI	430, 434, 570, 574
V	4	R11D1	CTCCATCGTTTTTTGTCGTTTTCTTC GTTTTTTTGGCACGCTTGTTCG	980	SspI	398, 582
V	12	F40D4	AATCGCACTTGCCGCTACTAAA GCACTGACAAATGACGGAACTT	1112	NruI	489, 623
V	25	W01F3	TTCCAACTGCTAACGACGGTCAA CGATTCTTTGAGCATCTCCATACA	1351	ApoI	652, 656, 695, 699
X	-20	R04A9	AAGAGTGAACCTTTTCCGTGAG TGATGCAATTTATACACACGCC	433	MseI	152, 154, 279, 281
X	-9	ZC64	TCTTCTTCTGGGATTACTTCGTCTTCA TTCCAATGTTACGCTACCAGCTTTTC	812	SspI	363, 449
X	-2	B0403*	CCTTTCCGTCCCACTTCTCAGTCT GGCTTGGAGGAAAATCATCAGGA	897	BglII	430, 434, 463, 467
X	2	T05A10	ATGCCAGTTCACAATCCCAATCC CATAAAATTCCAGAGAGGAGCGACG	1221	MfeI	551, 555, 666, 670
X	11	F46G10	CGAGAGAGATTCAGGACAACCAATAAAGT TTGAAAATAACTCCAATGATGTATGAA	713	AcuI	228, 230, 483, 485
X	24	F38E9	AAACTGGCTTCACGAAATGTAAAT ATTTGTCCTCACTAACTGTATGTCC	1231	HphI	612, 613, 618, 619

Results and Discussion:

Chromosomal and interval mapping of the known gene *dpy-5*

The validity of this method in mapping genes was verified by the mapping of an already cloned gene, *dpy-5*. Hermaphrodite worms from a marked mapping strain BA592 *dpy-5(e61)* I*; rol-1(e91)* II*; unc-32(e189)* III; were crossed to CB4856 males and a lysate was generated by selecting homozygous F2 Dpy progeny with a N2/CB4856 background. A lysate of worms from the BA592 parent strain was also made and serves as a control alongside N2 and CB4856.

To determine chromosomal linkage of *dpy-5(e61)*, the first round of analysis was performed using SNPs found at the center of the chromosomes as listed in Table 2.1. As expected, linkage to chromosome I was observed with no linkage to the other chromosomes (Figure 2.2).

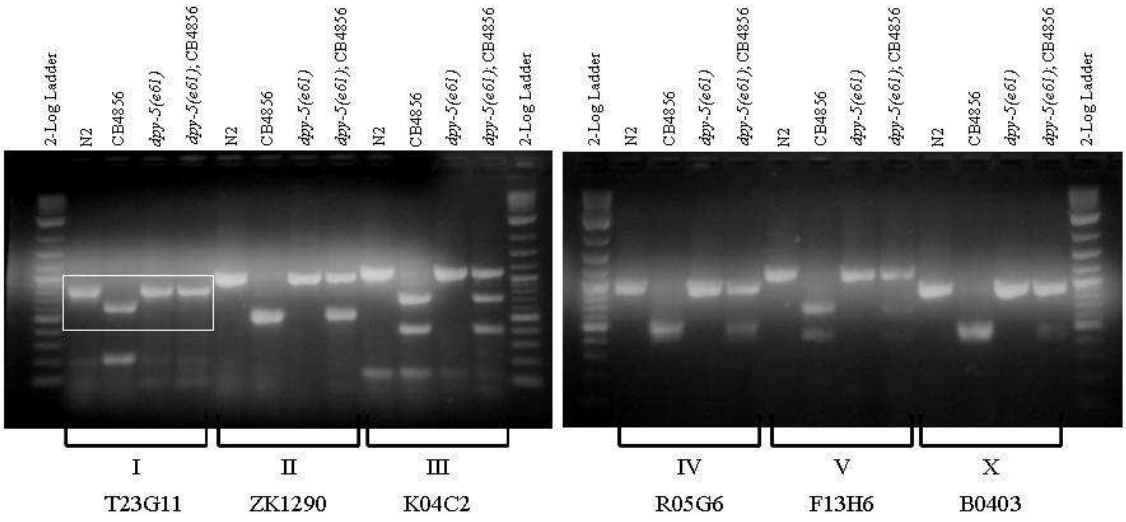

Figure 2.2: *dpy-5* chromosomal linkage. Results of restriction digest on PCR products of lysates from homozygous N2, CB4856, *dpy-5*, and *dpy-5*; CB4856 worms ran out on an agarose gel are shown. The SNP used for each chromosome is listed under each chromosome. Unlinked SNPs for recessive mutations will display an equal mix of N2 and CB4856 bands, whereas linked SNPs will display only N2 bands. Linkage to chromosome I is indicted by white box.

To identify the region on chromosome I that contains *dpy-5*, a second round of PCR and restriction digest analysis was performed. These results show that *dpy-5* is found towards the

middle of the chromosome, and is not located at the ends of chromosome I (Figure 2.3 A), as predicted.

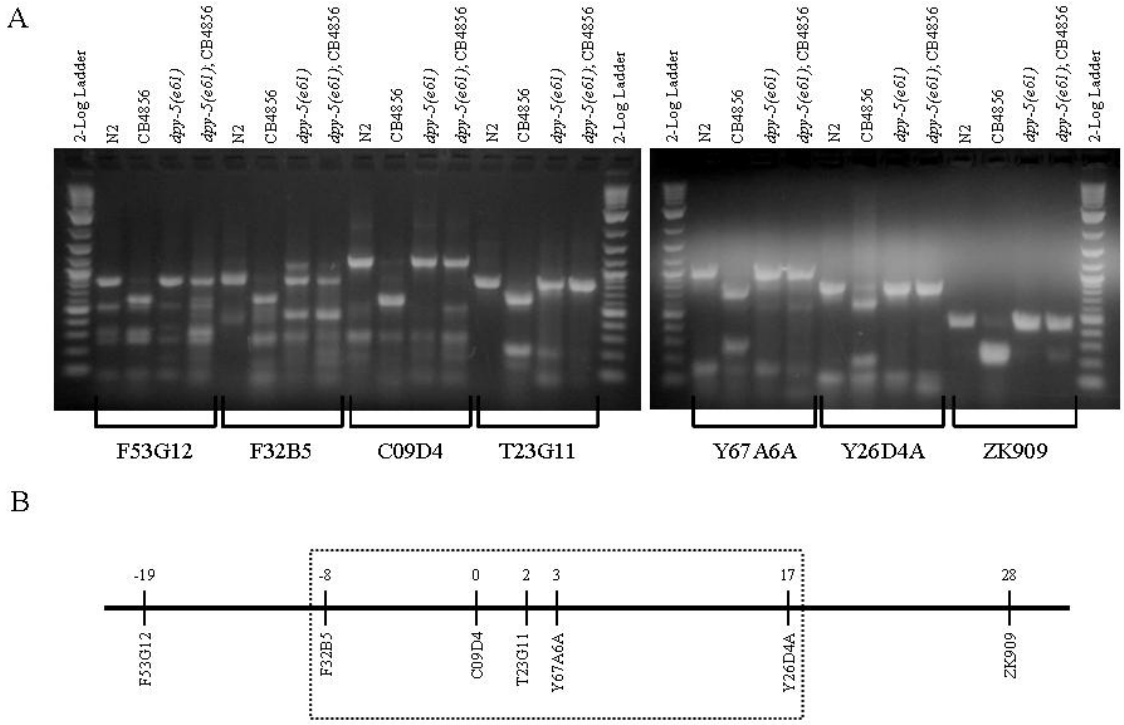

Figure 2.3: *dpy-5* interval mapping on chromosome I. A) Results of restriction digest on PCR products of lysates from homozygous N2, CB4856, *dpy-5*, and *dpy-5*; CB4856 worms ran out on an agarose gel are shown. The SNPs used are labeled at the bottom of the gel. Unlinked SNPs for recessive mutations will display an equal mix of N2 and CB4856 bands, whereas linked SNPs will display only N2 bands. B) Genetic positions of SNP markers on chromosome I with the region reported this data to contain *dpy-5* outlined by dashed lines.

The SNP markers outlined a region that centers around the middle of chromosome I where *dpy-5* is located (Figure 2.3 B). The published genetic position for *dpy-5* is zero, matching the region outlined by the SNP data. SNP markers within a chromosome provide boundaries allowing further, more in-depth mapping.

Chromosomal and interval mapping of an unknown mutation

Mapping of *as28*, an unknown mutation affecting fertilization in *C. elegans*, was performed to demonstrate the effectiveness of this method in initial gene mapping. Results from the

chromosomal linkage step were inconclusive in that linkage to a specific chromosome was not observed (Figure 2.4). Although linkage to a specific chromosome was not determined by this analysis, it does not demonstrate the failure of this method.

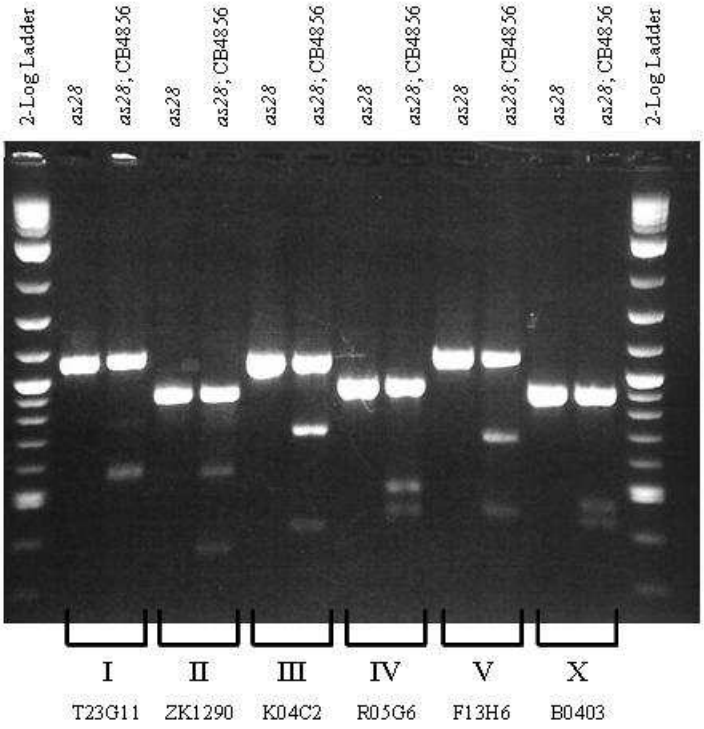

Figure 2.4: *as28* chromosomal linkage. Results of restriction digest on PCR products of lysates from homozygous *as28*, and *as28*; CB4856 worms ran out on an agarose gel are shown. The SNP used is listed under each chromosome. Unlinked SNPs will display N2 and digested CB4856 bands, whereas linked SNPs will display only an N2 band.

The *as28* mutation may be at the end of a chromosome, which would allow for the occurrence of recombination towards the middle of the chromosomes, where the SNP markers are located, resulting in band patterns that do not show linkage to any chromosome. To resolve this linkage issue, SNPs located at the ends of left and right arms of each chromosome were selected as markers to determine chromosome linkage. This analysis revealed linkage to the left arm of chromosome IV along with weak linkage to the right arm of chromosome III (Figure 2.5).

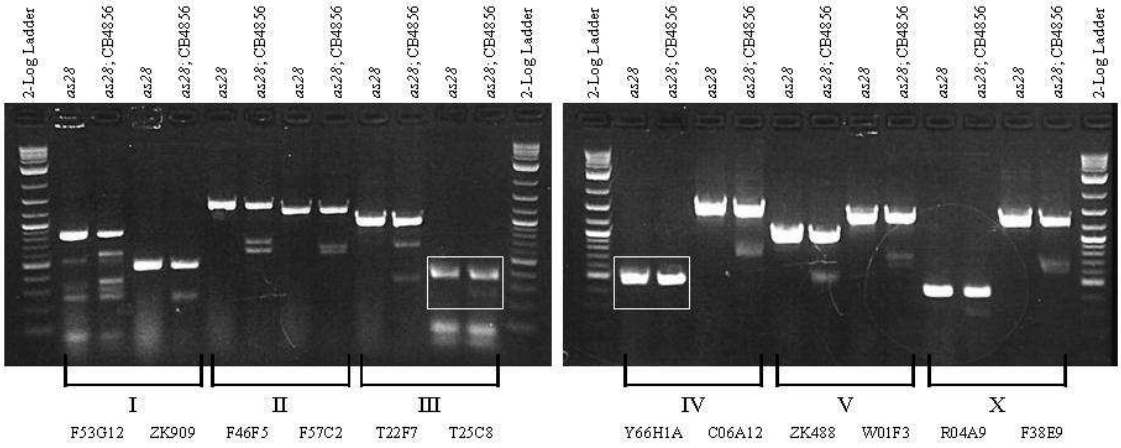

Figure 2.5: *as28* chromosomal linkage with SNP markers at ends of chromosomes. Results of restriction digest on PCR products of lysates from homozygous *as28*, and *as28*; CB4856 worms ran out on an agarose gel are shown. The SNPs used are listed under each chromosome. Unlinked SNPs will display N2 and digested CB4856 bands, whereas linked SNPs will display only an N2 band. Linkage to the left arm of chromosome IV and weak linkage to the right arm of chromosome III are indicted by white boxes.

Further analysis of SNP markers on chromosomes III and IV was performed to confirm linkage analysis and to narrow the region containing the gene with the *as28* mutation. For chromosome IV, the data shows clear-cut linkage to the upper most region of the left arm of the chromosome, with only N2 bands present and no CB4856 bands detected (Figure 2.6). For chromosome III, there is a digested CB4856 band present at the end of the right arm, but this band is fainter than the rest of the observed CB4856 digested bands on the same chromosome (Figure 2.6). The faint band could be a result of ineffective PCR cycles, contaminated samples, or the result of a dominant mutation. If the PCR cycles had errors, the resulting bands would not be as bright as bands resulting from error-free PCR cycles. Contaminated samples would contain CB4856 sequences, but not at a high concentration, would also result in fainter bands. Replicates of PCR and restriction digests contain the same faint band; therefore failed PCR or sample contamination does not explain this occurrence. Along with segregation ratios (56 sterile out of 457 total worms examined, 12.25%), the data suggest that the *as28* phenotype is a result of two mutations; a dominant mutation on the right arm of chromosome III, and a recessive mutation on the left arm of chromosome IV.

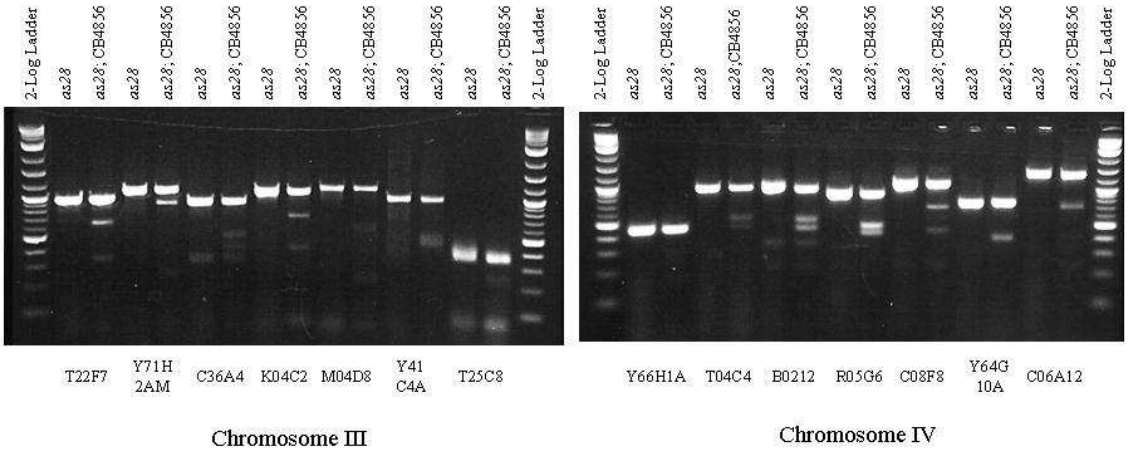

Figure 2.6: *as28* interval mapping with SNP markers from chromosomes III and IV. Results of restriction digest on PCR products of lysates from homozygous *as28*, and *as28*; CB4856 worms ran out on an agarose gel are shown. The SNPs used are labeled at the bottom of the gel. Unlinked SNPs will display N2 and digested CB4856 bands, whereas linked SNPs will display only an N2 band.

The multi-gene nature of the *as28* mutation makes it difficult to clone with current mapping strategies and technologies, making it a candidate for mutant allele identification with whole-genome sequencing.

Conclusion:

Despite the advantages of using SNPs in linkage and interval mapping over using physical markers in traditional linkage mapping, the use of SNP for linkage and interval is still not as widely practiced as physical markers. The previously published protocols are designed for mass-scale linkage and interval mapping, involving pin-replication [82] and automated robotic platforms [84]. However these conditions are not ideal for mapping of a single gene or smaller-scale analysis. The method presented in this work offers an advantage over previously published protocols [80, 82-84] for smaller-scale, individual cloning studies by providing a way to present mapping data in a clear-cut and unambiguous manner. The agarose gel banding patterns that result from this method make it easy to interpret the presence or absence of the out-crossed CB4856 sequences when compared to the endogenous N2 sequence. The results produced from this method do not pin-point a narrow region in which the mutation of interest is located, but

instead provides a general region for more fine-tuned mapping. This method can also be used to facilitate whole-genome sequencing for gene cloning or mutant allele identification for which fine scaled mapping is not required.

CHAPTER 3

Phenotypic characterization and mapping of a newly isolated temperature-sensitive mutation affecting fertilization in *Caenorhabditis elegans*

Introduction:

The transfer of genetic information to the next generation requires the formation of a zygote from two gametes. For fertilization to occur, sperm and oocyte must meet and interact with each other in a meaningful way. Sterility can result from many things, including the absence of sperm and/or oocytes, defective sperm development, activation, and function, or from defective oocyte development and/or maturation. Many of these processes have been described and studied in depth using model systems. However, a full understanding of how these processes coalesce for a successful fertilization event remains elusive; as there are many molecules and their roles have yet to be elucidated through these studies. *Caenorhabditis elegans* serves as an excellent paradigm for studying these potential factors that are involved in and events related to fertilization due to their rapid reproductive ability, along with real-time visualization of *in vivo* events.

Sperm activation, or spermiogenesis, is an important process by which immotile spermatids obtain motility to become mature spermatozoa. This phase of sperm differentiation occurs after the completion of meiosis. In *C. elegans*, the round, symmetrical spermatid acquires motility by generating a pseudopod. No mRNA molecules or proteins are synthesized during this process, yet the spermatid undergoes a dynamic morphological and physiological change to become a mature spermatozoa [4, 85].

It is speculated that multiple pathways are involved in regulating *C. elegans* sperm activation due to differences observed between hermaphrodites and male worms. In hermaphrodites, spermatids are activated upon entry into the spermatheca; whereas in males, spermatids are activated upon ejaculation and entry into the uterus [54]. The events of sperm activation for both male-derived and hermaphrodite-derived sperm are the same despite their different origins. During spermiogenesis, Major Sperm Protein (MSP), which is present in the fibrous bodies (FBs),

depolymerize to become the sperm cytoskeleton, and MSP is found to cluster at the pseudopod to facilitate sperm movement [86, 87]. Simultaneously, Golgi-derived membranous organelles (MOs) localize to and fuse with the plasma membrane [55]. This fusion allows the MOs to exocytose its contents on the sperm plasma membrane. The importance of MO fusion is delineated by defects that may occur during spermiogenesis. For example, defects in MO fusion result in spermatozoan with abnormally short pseudopods with motility defects, such as *spe-10* [87] and *fer-1* mutant sperm, which are unable to fertilize oocytes.

In this work, we present the phenotypic and linkage analysis for *as28*, a mutation that results in defective sperm activation. Hermaphrodite worms with the *as28* mutation are self-sterile due to a sperm specific defect. Both *as28* mutant males and hermaphrodites produce morphologically abnormal sperm that we hypothesize to be the result of defective MO fusion.

Methods:

Culturing of *C. elegans* strains

Culturing of *C. elegans* was done according to standard protocols described elsewhere [52]. The *as28* strain was maintained at 16°C and shifted to 25°C for experiments. The strains used in this work include: *as28*, *him-5(e1490)*, *dpy-5(e61)*, *rol-1(e91)*, *unc-32(e189)*, *unc-5(e52)*, *dpy-11(e224)*, *lon-2(e678)*, Bristol strain N2 (wild-type), and Hawaiian strain CB4856. Strains were obtained from the Caenorhabditis Genetics Center (CGC, University of Minnesota). The *as28* mutation was isolated from an ethyl methanesulfonate (EMS) mutagenesis screen conducted by Indrani Chatterjee and Emily Putiri; descriptions of all other strains can be found on Wormbase [1]. All strains were Bristol-derived except for the Hawaiian strain which was used in chromosomal linkage analysis. An *as28*;*him-5(e1490)* double mutant was created to increase the frequency of *as28* mutant males; for experiments involving this strain, the *him-5* strain is considered wild type.

Progeny and ovulation counts

The number of progeny for N2 (wild type) and *as28* was determined by placing individual worms on separate culture plates and counting an entire individual's brood. Ovulation rates were determined by combining the total number of embryos and unfertilized embryos laid during the entire lifetime of a worm [57, 64, 65, 86, 88]. Brood and ovulation counts were performed at 16°C, 20°C, and 25°C.

Germline morphology

Germline morphology for wild type and *as28* hermaphrodites was determined by mounting worms in 7μl 100μM NaN_3 onto 2% agarose slides for visualization with Nomarski imaging.

Sperm loss assay

The amount of sperm cell nuclei present in the spermatheca over a specified time period was examined to determine the rate of hermaphrodite sperm loss. Worms were fixed in cold methanol for 5 minutes, stained with 0.1μg/ml 4,6-diamidino-2-phenyl-indole (DAPI; Pierce) DNA binding dye, then mounted on 2% agarose slides for visualization under both Nomarski and fluorescence imaging.

Sperm isolation and *in vitro* activation

Sperm morphology and activation was assessed by previously describe methods [4, 85, 89]. The testis or spermatheca was dissected in 1X sperm media (SM) pH 7.8 with and without 200μg/ml Pronase, a known *in vitro* sperm activator [85]. To examine membranous organelle (MO) fusion, the fluorescent lipophilic styryl dye *N*-(3-triethylammoniumpropyl)-4-(4-(dibutylamino)styryl)pyridinium dibromide (FM 1-43; Molecular Probes) was added to 1X SM at

a concentration of 5μM to visualize membranes [90, 91]. Dissections of sperm were examined with both Nomarski and fluorescence imaging.

Genetic mapping

Initial chromosomal linkage mapping for *as28* was performed by crossing *as28* into two triply marked strains BA592 (*dpy-5(e61)* I; *rol-1(e91)* II; *unc-32(e189)* III) and MT464 (*unc-5(e62)* IV; *dpy-11(e224)* V; *lon-2(e678)* X). Results from these crosses were ambiguous, and an alternate technique was employed to determine chromosomal linkage. Chromosomal linkage for *as28* was determined by examining SNPs that result in a restriction fragment length polymorphism (RFLP) in the CB4856 Hawaiian strain. *as28* hermaphrodites were crossed to Hawaiian males at a ratio of 3 males to 1 hermaphrodite, the heterozygous progeny were allowed to self-fertilize, and F2 homozygous sterile progeny were isolated to generate a lysate which was analyzed for chromosomal linkage.

Results and Discussion:

***as28* mutant hermaphrodites are self-sterile**

as28, a newly isolated mutation, was uncovered in a screen for temperature sensitive sterile mutations. Brood counts showed that *as28* mutant animals have reduced fertility and decreased ovulation compared to wild type (N2) controls at the restrictive temperature of 25°C, with normal levels of fertility and ovulation at the permissive temperature of 16°C (Figure 3.1). This strain was determined to have sperm defects due to its ability to viable cross progeny when mated to wild-type males, indicating that there are no defects in oocytes produced by *as28* mutants. Heterozygous *as28*/+ worms are fertile, making *as28* a recessive mutation. Aside from the sterility, there are no other visible mutant phenotypes associated with *as28* animals; *as28* mutant hermaphrodites have wild-type morphology and appear to undergo spermatogenesis and

oogenesis normally (Figure 3.2). These observations suggest that the *as28* mutation only affects sperm.

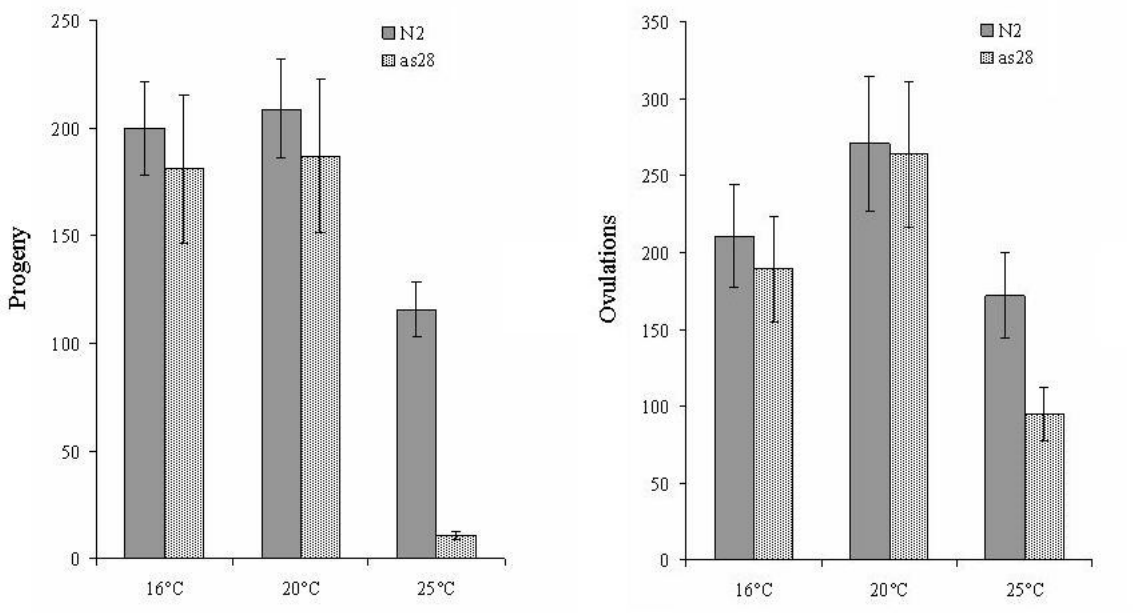

Figure 3.1: Brood and ovulation counts for unmated *as28* mutant hermaphrodites. *as28* animals have normal levels of fertility at lower temperatures (16°C and 20°C), but have greatly reduced fertility when shifted to a higher temperature (25°C). Ovulation rates are not affected in *as28* animals. n = 19-24 per allele.

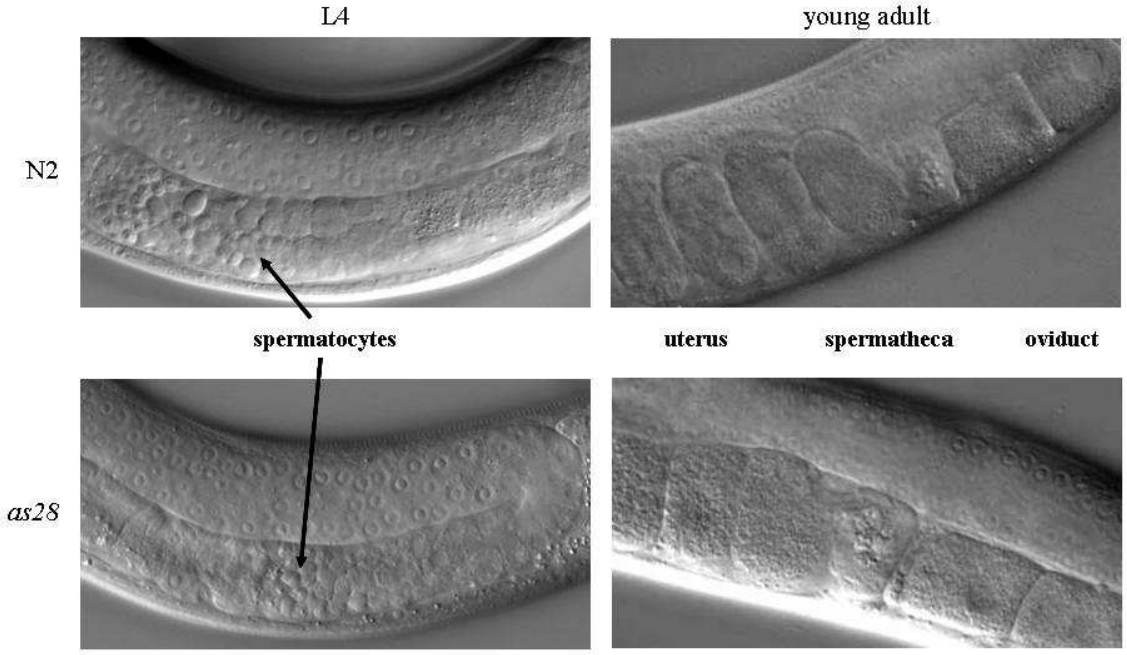

Figure 3.2: Nomarski DIC pictures of wild type and *as28* hermaphrodite germlines. *as28* mutant hermaphrodites appear to undergo spermatogenesis normally during the last larval stage, L4. *as28* mutant young adult hermaphrodites are sterile, with unfertilized oocytes present in their uteri, in contrast to the presence of developing embryos in wild-type uteri. Magnification at 60X.

as28 hermaphrodite-derived sperm are not maintained in the spermatheca

The ovulation rate for *as28* mutant hermaphrodites at the restrictive temperature of 25°C is slightly lower than that of wild-type animals. It has been shown that the presence of spermatids or spermatozoa in the spermatheca is needed for ovulation events to occur [92, 93]. To determine if the lower ovulation rate for *as28* mutant animals is a result of an inability to retain sperm in the spermatheca, age-matched DAPI-stained wild-type and *as28* mutant young adult hermaphrodites were examined for the presence of sperm cell nuclei in the spermatheca. The number of sperm present in the spermathecas of wild-type and *as28* mutant animals shortly after the animals reach adulthood at 25°C is comparable (Figure 3.3). However, in *as28* mutant young adults, there is a marked reduction in the number of visible sperm nuclei found in the spermatheca when compared to wild-type animals (Figure 3.3).

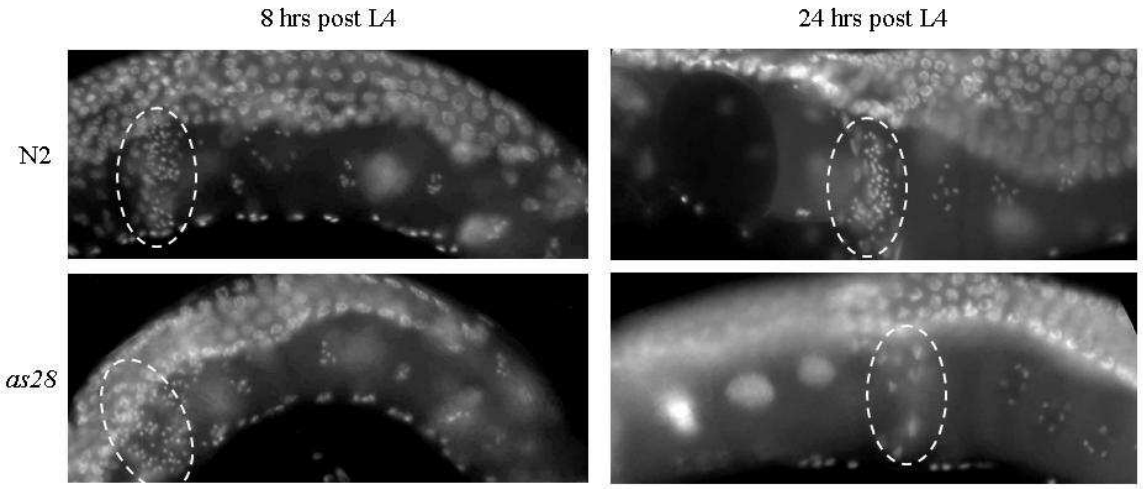

Figure 3.3: *as28* sperm loss phenotype. *as28* mutant sperm are lost from the reproductive tract and cannot fertilize oocytes. Dashed ovals denote the position of the spermatheca, sperm nuclei are visible as bright dots inside the spermatheca. Orientation of the reproductive tract from left to right is uterus, spermatheca, oviduct. Magnification at 60X.

These observations suggest the *as28* mutant sperm are unable to crawl back to the spermatheca after being swept into the uterus by passing oocytes. The absence of sperm in the mutant spermathecas could be the result of a defect in sperm activation resulting in mutant sperm that do not acquire full motility or it could be the mutant sperm are unable to properly sense the presence of the spermatheca and are unable to move towards the site.

as28 mutant animals produce morphologically abnormal spermatids

To characterize *as28* spermatids, dissections of wild-type (*him-5)* and *as28;him-5* males were performed and examined under Nomarski imaging. An *as28;him-5* double mutant strain was generated to increase the occurrence of males for dissections; the *him-5* mutation allows for an increase in the number of male progeny produced without generating any adverse effects on sperm [4]. Homozygous *as28;him-5* males produced spermatids that had an abnormal morphology (Figure 3.4) that remains unchanged after the addition of Pronase, a known sperm activator [85]. Sperm dissected from unmated *as28* mutant hermaphrodites have the same phenotype, suggesting that these mutant sperm do not undergo normal sperm activation. *as28* mutant spermatids have a distinctive cratered and vacuolated appearance as opposed to the smooth surface found on wild-type sperm, which could be the result of improperly fused MOs. Vacuolated spermatocytes have been observed in *spe-4* [94] and *spe-5* [95] mutants as a result of abnormal FB-MO development, but they rarely progress to become spermatids.

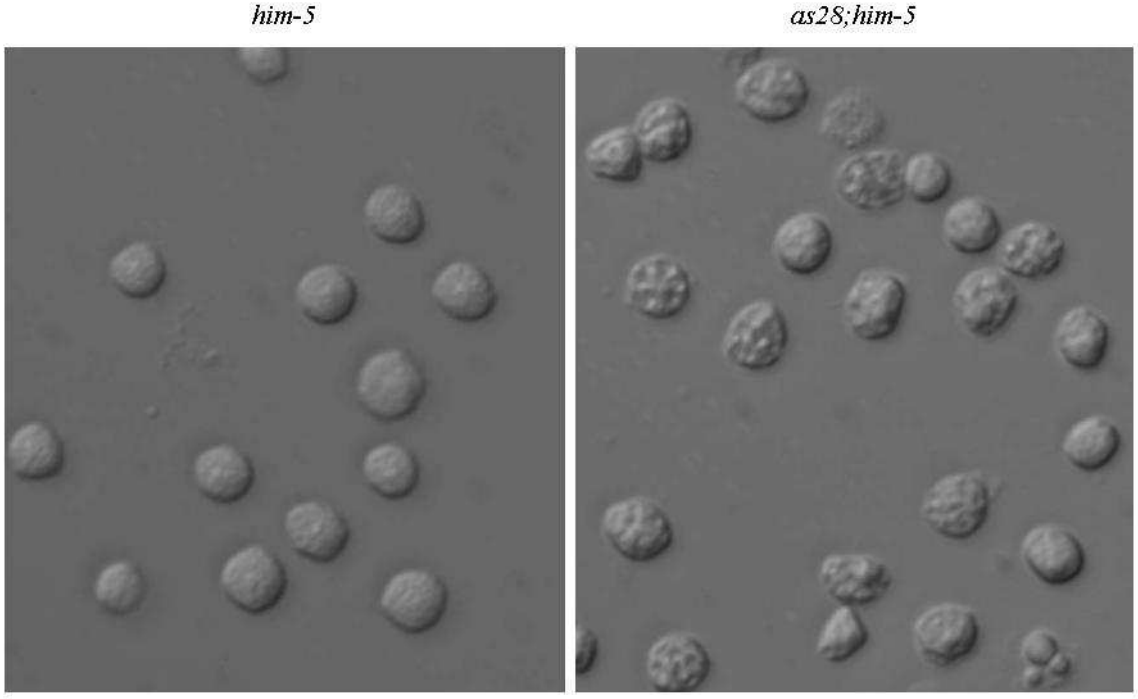

Figure 3.4: *as28* sperm activation phenotype. Spermatids derived from males were dissected in 1X sperm medium. Worms were grown at 25°C; L4 males were isolated the night before dissections for spermatid accumulation. Magnification at 100X.

To investigate the nature of the craters on *as28* mutant sperm, a fluorescent membrane marking dye, FM 1-43 (Molecular Probes), was used detect anomalies on the surfaces of spermatids and spermatozoa. FM 1-43 has been shown to be a potent marker of cell membrane surfaces [90], and an effective indicator for the presence of MOs on the sperm plasma membrane [91]. Wild-type spermatids visualized with FM 1-43 display a ring of fluorescence which corresponds to the spermatid plasma membrane. After activation, the MOs fuse with the plasma membrane and are concentrated on the cell body of the spermatozoa, which is observed as bright punctae in wild-type spermatozoa when dyed with FM 1-43; *fer-1* mutant sperm that have defective MO fusion with the plasma membrane do not contain these punctae, but instead have the same fluorescent ring seen in spermatids [91].

Spermatids derived from *as28;him-5* mutant males are not encircled by the fluorescent ring observed in wild-type spermatids (Figure 3.5). Instead, bright punctae associated with fused MOs are observed on the surface of *as28* spermatids that are normally observed with activated spermatozoa (Figure 3.5). These punctae, unlike the punctae on spermatozoa, are spread out and are not confined to a specific area. *as28;him-5* spermatids that are dissected in the presence of Pronase to undergo *in vitro* activation have the same characteristics as *as28* mutant spermatids dissected without Pronase. This data suggest that MO fusion does occur in *as28* mutant sperm, but it does so prematurely and asynchronous with activation cues. The fused MOs produce a cratered appearance on spermatids and prevent proper sperm activation.

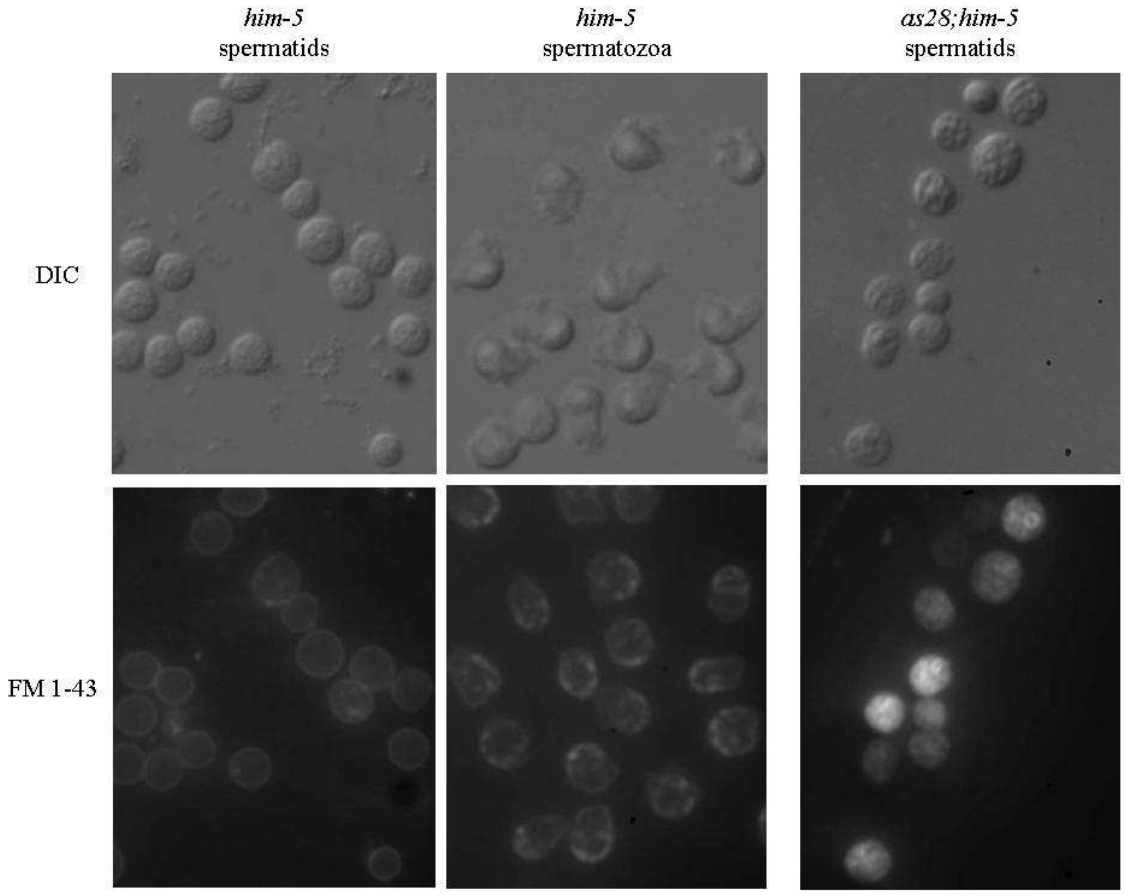

Figure 3.5: *as28* MO fusion phenotype. Sperm were dissected from males in 1X sperm medium + FM 1-43 and 1X sperm medium + FM 1-43 + Pronase. Magnification at 100X.

The *as28* phenotype is the result of two mutations

To identify and determine the nature of *as28*, genetic mapping was performed. Chromosomal linkage mapping was performed with the triply marked strains BA592 (*dpy-5(e61)* I; *rol-1(e91)* II; *unc-32(e189)* III) and MT464 (*unc-5(e52)* IV; *dpy-11(e224)* V; *lon-2(e678)* X) with ambiguous results. Tight linkage to a specific chromosome was not observed, instead weak linkage to Chromosomes III and IV was observed. To resolve this ambiguity, linkage was determined by a set of SNP markers that result in restriction fragment length polymorphisms. The *as28* mutant phenotype was found to be linked to regions on the right arm of chromosome III, and the left arm of chromosome IV. The segregation ratio for the *as28* mutant phenotype is approximately 1/8 or 12% (56 sterile out of 457 total animals examined) suggesting that it is not a

single recessive mutation; if this phenotype was the result of two recessive mutations, it would segregate at a ratio of 1/16 or 6%. Data from the SNP linkage analysis along with segregation ratios suggest that the *as28* mutant phenotype is the result of the combination of a dominant and a recessive mutation on Chromosome III and IV, respectively. Further analysis of *as28* segregation patterns would provide more insight into the genetic nature of this mutant phenotype.

Conclusion:

The multi-gene nature of the *as28* mutant phenotype makes it difficult to clone these genes with current mapping strategies and technologies, making them candidates for mutant allele identification with whole-genome sequencing. Once the genes are identified, it would be possible to generate antibodies and transgenic constructs to determine the cellular localization patterns of the protein products. Localization patterns and possible homology to known proteins will provide clues to the molecular function of the *as28* gene products. Epistatic analysis of the *as28* genes with other genes that have been shown to be involved in MO fusion, such as *spe-10* or *fer-1*, will provide insight into their positions in the MO fusion pathway and the relationship between these molecules.

Electron microscopy (EM) is needed to determine if the MOs in *as28* mutant sperm undergo fusion properly and to identify the observed vacuoles. EM analysis will also be able to detect any defects in *as28* mutant sperm that are not detected under light microscopy. The localization patterns of other MO fusion or sperm activation molecules in *as28* mutant will be observed to determine if their localization patterns and functions are altered. These observations could reveal relationships between the *as28* gene products and proteins known to be involved in sperm activation and MO fusion.

The cloning of the genes responsible for the *as28* mutant phenotype, and the subsequent characterization of the molecules involved, would shed more light on the elucidation of the role and method action of MO fusion during *C. elegans* sperm activation. These genes are unique in that the mutant phenotype is observed in both male- and hermaphrodite-derived sperm, and unlike many other FB-MO defective mutants, these sperm are able to mature to become spermatids. An interesting element is that these genes act in combination to produce the observed phenotype, and the cloning of these genes would identify a part of the MO fusion pathway involved in spermiogenesis. Gaining an understanding of the molecular mechanism of the pathways involved in sperm activation in *C. elegans* would provide insight for studies in other model systems due to the homologous and analogous nature of varying cell processes.

CHAPTER 4

Cloning of *spe-13*, a gene needed for sperm function during fertilization in *C. elegans*

Introduction:

Mutations that result in morphologically and physiologically normal sperm in *C. elegans* that are incapable of fertilizing oocytes are said to be sperm function mutations. Worms that have *spe-9* like mutations have small brood counts as a result of the defective sperm, but these worms ovulate at rates comparable to wild-type. Because of the normal morphology and physiology found in mutant sperm, it is hypothesized that the products of these genes are ligands or receptors needed for signaling to oocytes during fertilization. *spe-13*, one of the earlier genes discovered to belong to this class, remains uncloned; this work presents an update of the progress being made in an effort to clone this elusive gene.

Methods:

Culturing of *C. elegans* strains

Culturing of *C. elegans* was done according to standard protocols described elsewhere [52].The strains used in this work include: *spe-13(as8), spe-13(as9), spe-13(as31), spe-13(as32), spe-13(as33), spe-13(hc137),* and Bristol strain N2 (wild-type). Strains were obtained from the Caenorhabditis Genetics Center (CGC, University of Minnesota). Descriptions of all strains can be found on Wormbase [1]. All strains were Bristol-derived.

Progeny and ovulation counts

The number of progeny for N2 (wild type) and *spe-13(hc137)* was determined by placing individual worms on separate culture plates and counting an entire individual's brood. Ovulation rates were determined by combining the total number of embryos and unfertilized embryos laid during the entire lifetime of a worm [57, 64, 65, 86, 88]. Brood and ovulation counts were performed at 16°C and 25°C

Preparation of genomic DNA

Preparations of N2 and *spe-13(hc137)* genomic DNA were prepared according to a protocol modified from Andy Fire's lab that is publicly accessible (http://www.genetics.wustl.edu/tslab/Protocols/genomic_DNA_prep.htm). The genomic preps were then subjected to SOLiD sequencing (Applied Biosystems) for whole genome sequencing. Genomic DNA of other *spe-13* alleles, including *as8*, *as9*, *as31*, *as32*, and *as33* were prepared using the DNeasy Tissue Kit (Qiagen Cat# 69504). PCR of candidate genes was performed using allelic genomic DNA and the purified reaction products sent to Genewiz (South Plainfield, New Jersey) for sequencing.

Results and Discussion:

***spe-13* hermaphrodites are self-sterile at restrictive temperature**

Mutations in *spe-13* results in temperature sensitive hermaphrodites that are completely sterile at the restrictive temperature of 25°C and produce only a small number of progeny at the permissive temperature of 16°C (Figure 4.1). Of the *spe-13* alleles, *hc137* hermaphrodites produce more progeny at 16°C than the other, more recently generated, alleles. This discrepancy may be because the newer alleles may still contain extraneous mutations, as a result of the mutagenesis process, that may indirectly affect fertilization; whereas *hc137* has been in existence for more than 20 years and would have eliminated other mutations. The new alleles may also be the result of the same mutation or mutations that are in close proximity to each other.

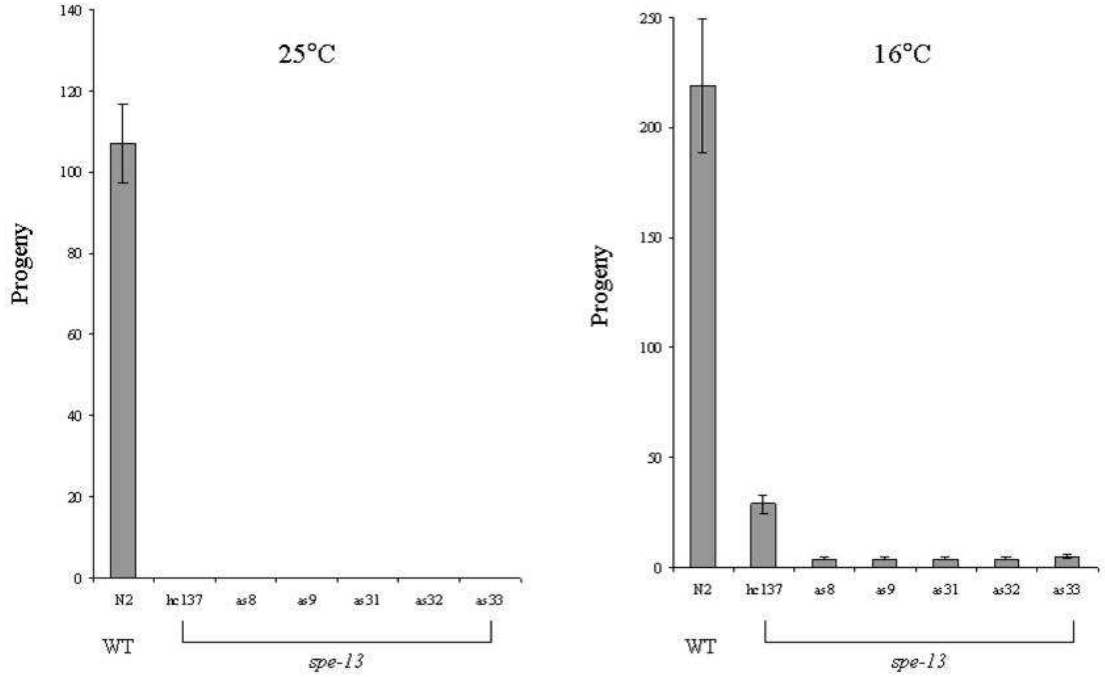

Figure 4.1: Brood counts for unmated *spe-13* mutant hermaphrodites at 25°C and 16°C. n = 20, 41-46 per allele.

Initial sequencing of *spe-13* candidate genes

Table 4.1: *spe-13* candidate genes.

Gene	Location on Chromosome I
F56C11.6	173412
C53D5.3	280120
Y65B4A.2	645454
Y18H1A.1	688282
Y18H1A.6 (pif-1)	720014
T06A4.2 (mps-3)	761838
Y95B8A.4	907467
Y95B8A.1 (nas-20)	942414
Y48G8AL.13	1229283

Candidate genes for *spe-13* were selected from the first 1.5 Mbp region on the left arm of Chromosome I based on their spermatogenesis-enriched expression patterns (Table 4.1). This region was chosen based on results of genetic mapping performed by Pavan Kadandale [96]. Sequences of these genes were generated and compared to wild-type (N2) and published sequences. Alignments of these sequences showed no differences in the *spe-13* sequences from wild-type sequences.

Verification of SNPs detected by SOLiD sequencing

Whole genome sequencing was employed to identify nucleotide differences between the *spe-13(hc137)* and wild-type (N2) genomes to facilitate the cloning of *spe-13*. SOLiD sequencing (Applied Biosystems) yielded 684 single nucleotide polymorphisms (SNPs) on Chromosome I between wild type and *spe-13(hc137)*. Out of that number there were eight promising SNPs in the first 2.5 Mbp region (Table 4.2). Sequencing of the other *spe-13* alleles determined that 6 of the 8 reported SNPs were deviations from the published sequence, but were not detected as deviations in the wild-type lab strain. The wild-type lab strain and the *spe-13* alleles contained the same nucleotide change for these candidates. Sequencing of the other two SNPs, in Y95B8A.6 and Y39G10AR.15, revealed true variants. For the SNP found in Y95B8A.6, sequencing of all *spe-13* alleles revealed that all of the *spe-13* alleles contained the same G to A change, with no other deviations or changes from wild type detected in the rest of the predicted gene. For the SNP found in Y39G10AR.15, only one allele, *spe-13(hc137)*, had the G to A change, the rest of the alleles had the published wild-type sequence at that position. There no were other changes detected in the predicted exons of Y39G10AR.15 (Figure 4.2).

Table 4.2: *spe-13* SNPs detected by SOLiD sequencing. *denotes SNPs that are true variants from the wild-type lab strain.

Physical Location	Nucleotide Change	Gene	Location of Change	Amino Acid Change
361325	C to A	R119.1	Exon	undetermined
732640	T to G	Y18H1A.15	Intron	N/A
887955	G to A*	Y95B8A.6	Exon	E59K
1074697	G to A	gsa-1	3' UTR	N/A
1089199	G to A	R06A10.5	Intron	N/A
1142103	C to A	Y48G8AL.10	Exon	undetermined
2326505	G to A*	Y39G10AR.15	Exon	E138K
2379643	C to T	Y39G10AR.17	Exon	undetermined

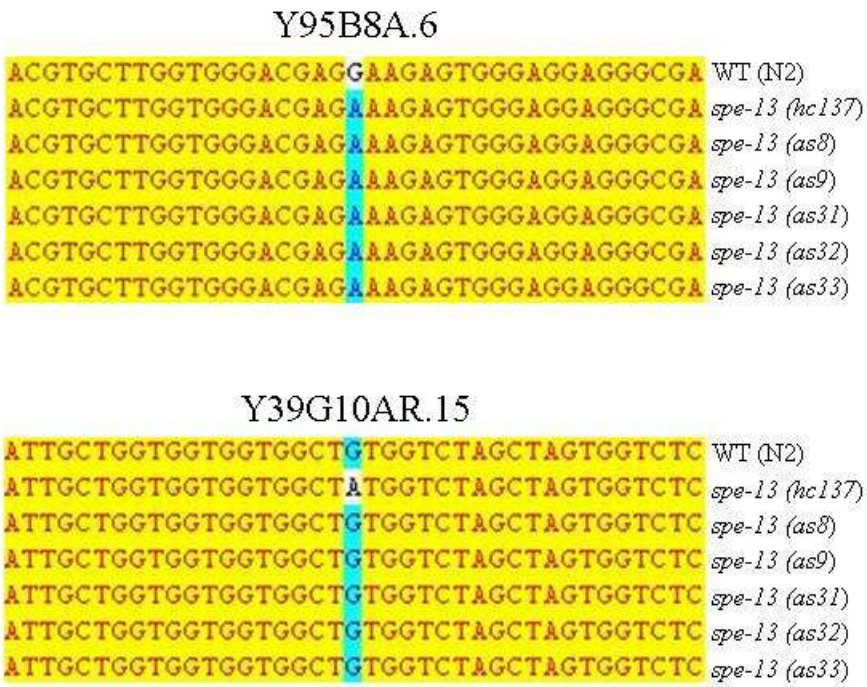

Figure 4.2: Sequence alignment of *spe-13* alleles for Y95B8A.6 and Y39G10AR.15.

The difference between the Y95B8A.6 and Y39G10AR.15 allelic sequencing results makes it difficult to discern which one contains the *spe-13* mutation. It could be possible that the *spe-13* mutation is very fastidious and that the mutant phenotype only results from a specific change at a specific nucleotide position, resulting in all of the alleles containing the same nucleotide change in the same position as in the Y95B8A.6 SNP. If this is the case, then the SNP found in Y39G10AR.15 could be the result of a change that is native to the strain that was mutagenized to create the *spe-13* mutation. It could be possible that the *spe-13* mutation is found in Y39G10AR.15, and that the deviations from the wild-type sequence in the other alleles have not been uncovered by sequencing of this gene's denoted exons and instead are found in the intronic sequence. Also, the exons in Y39G10AR.15 may not be accurately predicted, and the changes in the other alleles would be found in sequences that may be mislabeled as intronic or they may not be annotated as being part of the gene.

Conclusion:

In order to determine the gene that the *spe-13* mutation is in, transgenic rescue with constructs containing Y95B8A.6 and Y39G10AR.15 should be conducted. If one of these constructs is able to rescue the sterile phenotype found in *spe-13* mutant animals, then it can be conclusively established as the *spe-13* gene. Once the gene has been identified, its localization pattern will be determined via antibody staining, transgenic constructs, or with both methods. Localization patterns of other sperm function mutants with antibodies available (*spe-9*, *spe-38*, and *spe-41/trp-3*) in *spe-13* mutants should also be observed to determine if *spe-13* belongs to the same pathways that these proteins function in or if it is involved in a separate fertilization pathway in sperm. Searches for similar amino acid sequence in other species for homology should be conducted to establish if the protein is conserved between species and provide clues to its function. These further characterizations of the *spe-13* gene product after it has been identified will aid in determining its function and its role in *C. elegans* fertilization.

CHAPTER 5

Future directions

Contrary to popular belief that fertilization is one of the more defined and understood biological processes, the underlying molecular mechanism of fertilization still remains unknown. The events leading up to and including fertilization have been studied in many model systems, and therefore are well explained. However the molecules involved, their function, how they interact with each other, and how they drive the main fertilization event still remain unknown. With advances in biochemistry, forward and reverse genetics, it has become easier to manipulate and study molecules *in vitro* as well as *in vivo*. These advances combined with the use of genetic model systems, such as *C. elegans*, allow for a straightforward way to identify and determine the function of molecules involved in fertilization.

My work involved the characterization of a newly isolated mutation, *as28*, which results in worms that produce defective sperm that cannot complete fertilization. Linkage mapping of this mutant produced inconclusive results, which lead to the development of a set of SNP markers to determine *C. elegans* chromosomal linkage and interval mapping. The resulting method provides chromosomal linkage in an efficient and clear-cut manner. After performing linkage analysis with the SNP markers on *as28*, it was determined that the *as28* phenotype is in actuality due to two mutations. This discovery was surprising and presents a hurdle for the cloning of these genes. Whole genome sequencing would have to be utilized to clone these genes. Once these genes have been identified, experiments will be designed to determine the function and action of these gene products including determining the localization patterns for the gene products via GFP constructs and immunofluorescence. Homology searches based on the gene sequences will determine if there are homologs within other species.

Sperm derived from *as28* mutant animals have an abnormal cratered appearance that is hypothesized to be improperly fused membranous organelles (MOs). To determine if the vacuoles found on *as28* sperm are indeed prematurely fused MOs, immunofluorescence with 1CB4, a

known MO marker, will identify these vacuoles as MOs. Electron microscopy will need to be performed to definitively determine if the MOs are properly fused in *as28* mutant sperm. Images obtained from electron microscopy will also be able to detect any defects that are not visible under light microscopy.

It would also be of interest to examine the localization patterns of gene products that require the proper MO fusion products in *as28* sperm to see if their localization patterns are disrupted and if their function is impaired. If the vacuoles in *as28* are prematurely fused MOs, then the redistribution of SPE-38 and SPE-41/TRP-3 to the cell surface of activated sperm would not be affected. If they remain sequestered in the MOs of *as28* sperm and are not found on the sperm surface, then it would suggest that there may be defects in membrane trafficking. MO fusion and translocation has been hypothesized to trigger activation of these molecules. If these molecules are found to be inactive on the sperm surface, then it would suggest that MO fusion alone is an insufficient stimulus.

The fusion of sperm-oocyte membranes at fertilization is analogous to cell-cell fusion that occurs during other cellular processes, and the changes associated with *C. elegans* sperm activation could be similar to post-translational modifications that occur during cellular differentiation and morphogenesis. It is easier to study the molecules involved in processes that occur during fertilization due to the lack of other functions in sperm or oocytes that would be present in somatic cells. Manipulation of a single molecule in somatic cells could have an indirect impact on other unrelated processes due to the connectivity of the cellular processes. Results from experiments conducted in *C. elegans* can compliment data obtained in other model organisms to provide a general picture, as it may be easier to conduct certain experiments in specific model organisms compared to others.

The information gained from studying fertilization has real-world applications. Infertility is a prominent issue in our society; difficultly in conceiving has resulted in an entire industry focused on aiding people via assisted and *in vitro* reproduction techniques. Gaining a better understanding of the underlying molecular mechanism of fertilization may enable us to uncover the root causes of infertility develop treatments or alternative methods. This knowledge is not constricted to the realm of human infertility; there are numerous species of endangered species in captivity that are also facing reproductive issues. On the other hand, information gathered from studies of fertilization molecules may be used to generate novel contraceptive strategies designed at the molecular level. Also, contraceptive methods could be designed to control the overpopulation of animals.

The knowledge obtained from fertilization studies has a wide-range impact on other disciplines. This information would provide more insight into inter-cellular as well as intra-cellular interactions with the ultimate goal of obtaining an understanding of how these building blocks are arranged to create complex organisms. It is worth studying biological processes in model organisms even if the molecules and pathways are not conserved in other species; the information obtained about these molecules and pathways would provide us with general knowledge increasing our understanding of the world that we live in.

APPENDIX

List of primers, purpose, and location.

Primer stocks are at a concentration of 100 μM. Primer sequence and information can be found on the specification sheets in the binders labeled “oligos”.

Primer(s)	Purpose	Location
B0035	spe-36 SNP	Box 1
B0212	Linkage SNPs (working)	Box 2
B0403	Linkage SNPs (working)	Box 2
C05C12.1	spe-36 sequencing	spe-36 Candidate Primers
C05C12.5	spe-36 sequencing	spe-36 Candidate Primers
C06A12	Linkage SNPs (working)	Box 2
C08F8	Linkage SNPs (working)	Box 2
C09D4	Linkage SNPs (working)	Box 2
C10C6.3	spe-36 sequencing	spe-36 Candidate Primers
C16C8	Linkage SNPs (II - additional)	Box 3
C18H9	Linkage SNPs (II - additional)	Box 3
C30G12	Linkage SNPs (II - additional)	Box 3
C36A4	Linkage SNPs (III - additional)	Box 3
C44E1	Linkage SNPs (test)	Box 1
C50F4	Linkage SNPs (working)	Box 2
C53D5.3	spe-13 sequencing	spe-13 Candidate Primers Box 3
D1022	Linkage SNPs (working)	Box 2
EEED8	Linkage SNPs (test)	Julie Primers Box 1
F08B1	Linkage SNPs (II - additional)	Box 3
F09C6	Linkage SNPs (test)	Julie Primers Box 1
F09D1	Linkage SNPs (test)	Julie Primers Box 1
F13H6	Linkage SNPs (working)	Box 2
F25F2	Linkage SNPs (working)	Box 2
F32B5	Linkage SNPs (working)	Box 2
F35B3	Linkage SNPs (test)	Julie Primers Box 1
F35F10	Linkage SNPs (working)	Box 2
F37B12	Linkage SNPs (II - additional)	Box 3
F37H8	Linkage SNPs (II - additional)	Box 3
F38E9	Linkage SNPs (working)	Box 3
F40D4	Linkage SNPs (test)	Box 1
F43C11	Linkage SNPs (test)	Box 1
F46F5	Linkage SNPs (working)	Box 2
F46G10	Linkage SNPs (working)	Box 2
F48F5	Linkage SNPs (test)	Box 1

Primer(s)	Purpose	Location
F53G12	spe-13 sequencing	spe-13 Candidate Primers Box 3
F53G12	Linkage SNPs (working)	Box 2
F54D1	spe-36 SNP	Box 1
F54D1.1	spe-36 sequencing	spe-36 Candidate Primers
F54D10	Linkage SNPs (II - additional)	Box 3
F56C11.6	spe-13 sequencing	spe-13 Candidate Primers Box 3
F57C2	Linkage SNPs (working)	Box 2
F57G8	Linkage SNPs (test)	Box 1
gsa-1_R06A10.3	spe-13 sequencing (SOLiD)	Box 3
K04C2	Linkage SNPs (working)	Box 2
K05F1	Linkage SNPs (working)	Box 2
K12B6	Linkage SNPs (test)	Box 1
M03A1	Linkage SNPs (II - additional)	Box 3
M04B2	spe-36 SNP	Box 1
M04D8	Linkage SNPs (working)	Box 2
mep-1	spe-36 comp testing	Box 1
ok300	spe-36 comp testing	Box 1
ok375	spe-36 comp testing	Box 1
ok421	spe-36 comp testing	Box 1
ok750	spe-36 comp testing	Box 1
q660	spe-36 comp testing	Box 1
R04A9	Linkage SNPs (working)	Box 2
R05G6	Linkage SNPs (working)	Box 2
R06A10.5	spe-13 sequencing (SOLiD)	Box 3
R119.1	spe-13 sequencing (SOLiD)	Box 3
R11D1	Linkage SNPs (working)	Box 2
T04C4	Linkage SNPs (working)	Box 2
T05A10	Linkage SNPs (working)	Box 2
T06A10	Linkage SNPs (test)	Julie Primers Box 1
T06A4.2	spe-13 sequencing	spe-13 Candidate Primers Box 1
T06A4.2	spe-13 sequencing (SOLiD)	Box 3
T13H5	Linkage SNPs (II - additional)	Box 3
T17A3	Linkage SNPs (test)	Box 1
T22F7	Linkage SNPs (working)	Box 2
T23G11	Linkage SNPs (working)	Box 2
T23G7	Linkage SNPs (II - additional)	Box 3
T24H10	Linkage SNPs (working)	Box 2
T25C8	Linkage SNPs (working)	Box 2
T25D3	Linkage SNPs (test)	Box 1
T25D3b	Linkage SNPs (test)	Box 1
T28D6	Linkage SNPs (test)	Box 1
tm1049	spe-36 comp testing	Box 1
tm1191	egg-3 sequencing	Box 1
tm1463	spe-36 comp testing	Box 1

Primer(s)	Purpose	Location
tm1855	spe-36 comp testing	Box 1
tm446	spe-36 comp testing	Box 1
tm464	spe-36 comp testing	Box 1
tm566	spe-36 comp testing	Box 1
W01F3	Linkage SNPs (working)	Box 2
W10G11	Linkage SNPs (II - additional)	Box 3
Y18H1A.1	spe-13 sequencing	spe-13 Candidate Primers Box 1
Y18H1A.15	spe-13 sequencing	spe-13 Candidate Primers Box 2
Y18H1A.6	spe-13 sequencing	spe-13 Candidate Primers Box 1
Y18H1A.6	spe-13 sequencing (SOLiD)	Box 3
Y25C1A	Linkage SNPs (test)	Box 1
Y26D4A	Linkage SNPs (working)	Box 2
Y37A1B	Linkage SNPs (test)	Box 1
Y38C9B	Linkage SNPs (test)	Box 1
Y39G10AR.15	spe-13 sequencing (SOLiD)	Box 3
Y39G10AR.17	spe-13 sequencing (SOLiD)	Box 3
Y41C4A	Linkage SNPs (working)	Box 2
Y41D4A	Linkage SNPs (test)	Box 1
Y47D3A	Linkage SNPs (test)	Box 1
Y48G8AL.10	spe-13 sequencing (SOLiD)	Box 3
Y48G8AL.13	spe-13 sequencing	spe-13 Candidate Primers Box 2
Y49F6A	Linkage SNPs (II - additional)	Box 3
Y51H1A	Linkage SNPs (test)	Box 1
Y57A10A	Linkage SNPs (working)	Box 2
Y64G10A	Linkage SNPs (working)	Box 2
Y65B4A.2	spe-13 sequencing	spe-13 Candidate Primers Box 2
Y66H1A	Linkage SNPs (working)	Box 2
Y67A6A	Linkage SNPs (working)	Box 2
Y71H2AM	Linkage SNPs (working)	Box 2
Y95B8A.1	spe-13 sequencing	spe-13 Candidate Primers Box 3
Y95B8A.3	spe-13 sequencing	spe-13 Candidate Primers Box 3
Y95B8A.4	spe-13 sequencing	spe-13 Candidate Primers Box 3
Y95B8A.6	spe-13 sequencing (SOLiD)	Box 3
ZC64	Linkage SNPs (working)	Box 2
ZK1290	Linkage SNPs (working)	Box 2
ZK488	Linkage SNPs (working)	Box 2
ZK666	Linkage SNPs (II - additional)	Box 3
ZK809	spe-36 SNP	Box 1
ZK809.1	spe-36 sequencing	spe-36 Candidate Primers
ZK909	Linkage SNPs (working)	Box 2
T28D6	Linkage SNPs (test)	Box 1
tm1049	spe-36 comp testing	Box 1
tm1191	egg-3 sequencing	Box 1
tm1463	spe-36 comp testing	Box 1

spe-36 mapping

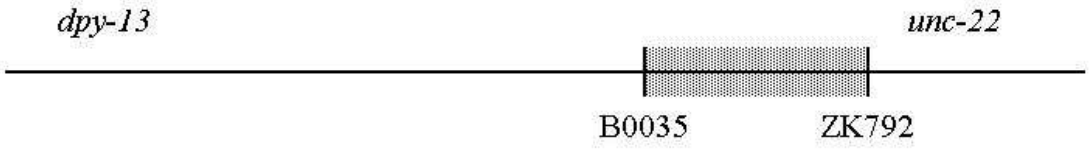

SNP mapping of *spe-36* has it being found in a 341kb region (indicated by the dashed region in figure) on chromosome IV between the SNPs B0035 and ZK792 (physical positions of 11,327,085 and 11,668,085, respectively). A doubly marked strain (*dpy-13 spe-36 unc-22)* was created for SNP mapping.

BIBLIOGRAPHY

1. Rogers, A., Antoshechkin, I., Bieri, T., Blasiar, D., Bastiani, C., Canaran, P., Chan, J., Chen, W.J., Davis, P., Fernandes, J., Fiedler, T.J., Han, M., Harris, T.W., Kishore, R., Lee, R., McKay, S., Muller, H.M., Nakamura, C., Ozersky, P., Petcherski, A., Schindelman, G., Schwarz, E.M., Spooner, W., Tuli, M.A., Van Auken, K., Wang, D., Wang, X., Williams, G., Yook, K., Durbin, R., Stein, L.D., Spieth, J., and Sternberg, P.W. (2008). WormBase 2007. Nucleic Acids Res *36*, D612-617.

2. Evans, J.P., and Florman, H.M. (2002). The state of the union: the cell biology of fertilization. Nat Cell Biol *4 Suppl*, s57-63.

3. Evans, J.P., and Kopf, G.S. (1998). Molecular mechanisms of sperm-egg interactions and egg activation. Andrologia *30*, 297-307.

4. Nelson, G.A., and Ward, S. (1980). Vesicle fusion, pseudopod extension and amoeboid motility are induced in nematode spermatids by the ionophore monensin. Cell *19*, 457-464.

5. Primakoff, P., and Myles, D.G. (2002). Penetration, adhesion, and fusion in mammalian sperm-egg interaction. Science *296*, 2183-2185.

6. Singson, A. (2001). Every sperm is sacred: fertilization in Caenorhabditis elegans. Dev Biol *230*, 101-109.

7. Talbot, P., Shur, B.D., and Myles, D.G. (2003). Cell adhesion and fertilization: steps in oocyte transport, sperm-zona pellucida interactions, and sperm-egg fusion. Biol Reprod *68*, 1-9.

8. Wassarman, P.M. (1999). Mammalian fertilization: molecular aspects of gamete adhesion, exocytosis, and fusion. Cell *96*, 175-183.

9. Wassarman, P.M., Jovine, L., and Litscher, E.S. (2001). A profile of fertilization in mammals. Nat Cell Biol *3*, E59-64.

10. Breitbart, H., Cohen, G., and Rubinstein, S. (2005). Role of actin cytoskeleton in mammalian sperm capacitation and the acrosome reaction. Reproduction *129*, 263-268.

11. Rubinstein, E., Ziyyat, A., Wolf, J.P., Le Naour, F., and Boucheix, C. (2006). The molecular players of sperm-egg fusion in mammals. Semin Cell Dev Biol *17*, 254-263.

12. Singson, A., Zannoni, S., and Kadandale, P. (2001). Molecules that function in the steps of fertilization. Cytokine Growth Factor Rev *12*, 299-304.

13. Bohmer, M., Van, Q., Weyand, I., Hagen, V., Beyermann, M., Matsumoto, M., Hoshi, M., Hildebrand, E., and Kaupp, U.B. (2005). Ca2+ spikes in the flagellum control chemotactic behavior of sperm. Embo J *24*, 2741-2752.

14. Nishigaki, T., Chiba, K., Miki, W., and Hoshi, M. (1996). Structure and function of asterosaps, sperm-activating peptides from the jelly coat of starfish eggs. Zygote *4*, 237-245.

15. Suzuki, N., Shimomura, H., Radany, E.W., Ramarao, C.S., Ward, G.E., Bentley, J.K., and Garbers, D.L. (1984). A peptide associated with eggs causes a mobility shift in a major plasma membrane protein of spermatozoa. J Biol Chem *259*, 14874-14879.

16. Ward, G.E., Brokaw, C.J., Garbers, D.L., and Vacquier, V.D. (1985). Chemotaxis of Arbacia punctulata spermatozoa to resact, a peptide from the egg jelly layer. J Cell Biol *101*, 2324-2329.

17. Hildebrand, E., and Kaupp, U.B. (2005). Sperm chemotaxis: a primer. Ann N Y Acad Sci *1061*, 221-225.

18. Schultz, R., and Williams, C. (2005). Developmental biology: sperm-egg fusion unscrambled. Nature *434*, 152-153.

19. Bleil, J.D., and Wassarman, P.M. (1980). Mammalian sperm-egg interaction: identification of a glycoprotein in mouse egg zonae pellucidae possessing receptor activity for sperm. Cell *20*, 873-882.

20. Primakoff, P., Hyatt, H., and Tredick-Kline, J. (1987). Identification and purification of a sperm surface protein with a potential role in sperm-egg membrane fusion. J Cell Biol *104*, 141-149.

21. Cho, C., Bunch, D.O., Faure, J.E., Goulding, E.H., Eddy, E.M., Primakoff, P., and Myles, D.G. (1998). Fertilization defects in sperm from mice lacking fertilin beta. Science *281*, 1857-1859.

22. Almeida, E.A., Huovila, A.P., Sutherland, A.E., Stephens, L.E., Calarco, P.G., Shaw, L.M., Mercurio, A.M., Sonnenberg, A., Primakoff, P., Myles, D.G., and White, J.M. (1995). Mouse egg integrin alpha 6 beta 1 functions as a sperm receptor. Cell *81*, 1095-1104.

23. Chen, H., and Sampson, N.S. (1999). Mediation of sperm-egg fusion: evidence that mouse egg alpha6beta1 integrin is the receptor for sperm fertilinbeta. Chem Biol *6*, 1-10.

24. Takahashi, Y., Bigler, D., Ito, Y., and White, J.M. (2001). Sequence-specific interaction between the disintegrin domain of mouse ADAM 3 and murine eggs: role of beta1 integrin-associated proteins CD9, CD81, and CD98. Mol Biol Cell *12*, 809-820.

25. Miller, B.J., Georges-Labouesse, E., Primakoff, P., and Myles, D.G. (2000). Normal fertilization occurs with eggs lacking the integrin alpha6beta1 and is CD9-dependent. J Cell Biol *149*, 1289-1296.

26. Linder, B., and Heinlein, U.A. (1997). Decreased in vitro fertilization efficiencies in the presence of specific cyritestin peptides. Dev Growth Differ *39*, 243-247.

27. Yuan, R., Primakoff, P., and Myles, D.G. (1997). A role for the disintegrin domain of cyritestin, a sperm surface protein belonging to the ADAM family, in mouse sperm-egg plasma membrane adhesion and fusion. J Cell Biol *137*, 105-112.

28. Shamsadin, R., Adham, I.M., Nayernia, K., Heinlein, U.A., Oberwinkler, H., and Engel, W. (1999). Male mice deficient for germ-cell cyritestin are infertile. Biol Reprod *61*, 1445-1451.

29. Inoue, N., Ikawa, M., Isotani, A., and Okabe, M. (2005). The immunoglobulin superfamily protein Izumo is required for sperm to fuse with eggs. Nature *434*, 234-238.

30. Chen, M.S., Tung, K.S., Coonrod, S.A., Takahashi, Y., Bigler, D., Chang, A., Yamashita, Y., Kincade, P.W., Herr, J.C., and White, J.M. (1999). Role of the integrin-associated protein CD9 in binding between sperm ADAM 2 and the egg integrin alpha6beta1: implications for murine fertilization. Proc Natl Acad Sci U S A *96*, 11830-11835.

31. Le Naour, F., Rubinstein, E., Jasmin, C., Prenant, M., and Boucheix, C. (2000). Severely reduced female fertility in CD9-deficient mice. Science *287*, 319-321.

32. Miyado, K., Yoshida, K., Yamagata, K., Sakakibara, K., Okabe, M., Wang, X., Miyamoto, K., Akutsu, H., Kondo, T., Takahashi, Y., Ban, T., Ito, C., Toshimori, K., Nakamura, A., Ito, M., Miyado, M., Mekada, E., and Umezawa, A. (2008). The fusing ability of sperm is bestowed by CD9-containing vesicles released from eggs in mice. Proc Natl Acad Sci U S A *105*, 12921-12926.

33. Miyado, K., Yamada, G., Yamada, S., Hasuwa, H., Nakamura, Y., Ryu, F., Suzuki, K., Kosai, K., Inoue, K., Ogura, A., Okabe, M., and Mekada, E. (2000). Requirement of CD9 on the egg plasma membrane for fertilization. Science *287*, 321-324.

34. Rubinstein, E., Le Naour, F., Lagaudriere-Gesbert, C., Billard, M., Conjeaud, H., and Boucheix, C. (1996). CD9, CD63, CD81, and CD82 are components of a surface tetraspan network connected to HLA-DR and VLA integrins. Eur J Immunol *26*, 2657-2665.

35. Coonrod, S.A., Naaby-Hansen, S., Shetty, J., Shibahara, H., Chen, M., White, J.M., and Herr, J.C. (1999). Treatment of mouse oocytes with PI-PLC releases 70-kDa (pI 5) and 35- to 45-kDa (pI 5.5) protein clusters from the egg surface and inhibits sperm-oolemma binding and fusion. Dev Biol *207*, 334-349.

36. Miyazaki, S., and Ito, M. (2006). Calcium signals for egg activation in mammals. J Pharmacol Sci *100*, 545-552.

37. Stricker, S.A. (1999). Comparative biology of calcium signaling during fertilization and egg activation in animals. Dev Biol *211*, 157-176.

38. Miyazaki, S., Shirakawa, H., Nakada, K., and Honda, Y. (1993). Essential role of the inositol 1,4,5-trisphosphate receptor/Ca2+ release channel in Ca2+ waves and Ca2+ oscillations at fertilization of mammalian eggs. Dev Biol *158*, 62-78.

39. Tsaadon, A., Eliyahu, E., Shtraizent, N., and Shalgi, R. (2006). When a sperm meets an egg: block to polyspermy. Mol Cell Endocrinol *252*, 107-114.

40. Swann, K., Saunders, C.M., Rogers, N.T., and Lai, F.A. (2006). PLCzeta(zeta): a sperm protein that triggers Ca2+ oscillations and egg activation in mammals. Semin Cell Dev Biol *17*, 264-273.

41. Fissore, R.A., Gordo, A.C., and Wu, H. (1998). Activation of development in mammals: is there a role for a sperm cytosolic factor? Theriogenology *49*, 43-52.

42. Homa, S.T., and Swann, K. (1994). A cytosolic sperm factor triggers calcium oscillations and membrane hyperpolarizations in human oocytes. Hum Reprod *9*, 2356-2361.

43. Swann, K. (1990). A cytosolic sperm factor stimulates repetitive calcium increases and mimics fertilization in hamster eggs. Development *110*, 1295-1302.

44. Tang, T.S., Dong, J.B., Huang, X.Y., and Sun, F.Z. (2000). Ca(2+) oscillations induced by a cytosolic sperm protein factor are mediated by a maternal machinery that functions only once in mammalian eggs. Development *127*, 1141-1150.

45. Galione, A., and Churchill, G.C. (2002). Interactions between calcium release pathways: multiple messengers and multiple stores. Cell Calcium *32*, 343-354.

46. Jones, K.T., Cruttwell, C., Parrington, J., and Swann, K. (1998). A mammalian sperm cytosolic phospholipase C activity generates inositol trisphosphate and causes Ca2+ release in sea urchin egg homogenates. FEBS Lett *437*, 297-300.

47. Saunders, C.M., Larman, M.G., Parrington, J., Cox, L.J., Royse, J., Blayney, L.M., Swann, K., and Lai, F.A. (2002). PLC zeta: a sperm-specific trigger of Ca(2+) oscillations in eggs and embryo development. Development *129*, 3533-3544.

48. Yoda, A., Oda, S., Shikano, T., Kouchi, Z., Awaji, T., Shirakawa, H., Kinoshita, K., and Miyazaki, S. (2004). Ca2+ oscillation-inducing phospholipase C zeta expressed in mouse eggs is accumulated to the pronucleus during egg activation. Dev Biol *268*, 245-257.

49. Kurokawa, M., Sato, K., Wu, H., He, C., Malcuit, C., Black, S.J., Fukami, K., and Fissore, R.A. (2005). Functional, biochemical, and chromatographic characterization of the complete [Ca2+]i oscillation-inducing activity of porcine sperm. Dev Biol *285*, 376-392.

50. Cox, L.J., Larman, M.G., Saunders, C.M., Hashimoto, K., Swann, K., and Lai, F.A. (2002). Sperm phospholipase Czeta from humans and cynomolgus monkeys triggers Ca2+ oscillations, activation and development of mouse oocytes. Reproduction *124*, 611-623.

51. Nomikos, M., Blayney, L.M., Larman, M.G., Campbell, K., Rossbach, A., Saunders, C.M., Swann, K., and Lai, F.A. (2005). Role of phospholipase C-zeta domains in Ca2+-dependent phosphatidylinositol 4,5-bisphosphate hydrolysis and cytoplasmic Ca2+ oscillations. J Biol Chem *280*, 31011-31018.

52. Brenner, S. (1974). The genetics of Caenorhabditis elegans. Genetics *77*, 71-94.

53. Ward, S., and Carrel, J.S. (1979). Fertilization and sperm competition in the nematode Caenorhabditis elegans. Dev Biol *73*, 304-321.

54. Ward, S., Hogan, E., and Nelson, G.A. (1983). The initiation of spermiogenesis in the nematode Caenorhabditis elegans. Dev Biol *98*, 70-79.

55. L'Hernault S, W. (2006). Spermatogenesis. In *Wormbook*, ed., T.*C.e.*R. Community, ed.

56. LaMunyon, C.W., and Ward, S. (1995). Sperm precedence in a hermaphroditic nematode (Caenorhabditis elegans) is due to competitive superiority of male sperm. Experientia *51*, 817-823.

57. Singson, A., Hill, K.L., and L'Hernault, S.W. (1999). Sperm competition in the absence of fertilization in Caenorhabditis elegans. Genetics *152*, 201-208.

58. Schedl, T. (1997). Developmental Genetics of the Germ Line. In C. Elegans II, D.L. Riddle, T. Blumenthal, B.J. Meyer and J.R. Priess, eds. (Cold Spring Harbor: Cold Spring Harbor Laboratory Press), pp. 241-269.

59. L'Hernault, S.W., Shakes, D.C., and Ward, S. (1988). Developmental genetics of chromosome I spermatogenesis-defective mutants in the nematode Caenorhabditis elegans. Genetics *120*, 435-452.

60. Singson, A., Mercer, K.B., and L'Hernault, S.W. (1998). The C. elegans spe-9 gene encodes a sperm transmembrane protein that contains EGF-like repeats and is required for fertilization. Cell *93*, 71-79.

61. Zannoni, S., L'Hernault, S.W., and Singson, A.W. (2003). Dynamic localization of SPE-9 in sperm: a protein required for sperm-oocyte interactions in Caenorhabditis elegans. BMC Dev Biol *3*, 10.

62. Putiri, E., Zannoni, S., Kadandale, P., and Singson, A. (2004). Functional domains and temperature-sensitive mutations in SPE-9, an EGF repeat-containing protein required for fertility in Caenorhabditis elegans. Dev Biol *272*, 448-459.

63. Davis, C.G. (1990). The many faces of epidermal growth factor repeats. New Biol *2*, 410-419.

64. Chatterjee, I., Richmond, A., Putiri, E., Shakes, D.C., and Singson, A. (2005). The Caenorhabditis elegans spe-38 gene encodes a novel four-pass integral membrane protein required for sperm function at fertilization. Development *132*, 2795-2808.

65. Xu, X.Z., and Sternberg, P.W. (2003). A C. elegans sperm TRP protein required for sperm-egg interactions during fertilization. Cell *114*, 285-297.

66. Kroft, T.L., Gleason, E.J., and L'Hernault, S.W. (2005). The spe-42 gene is required for sperm-egg interactions during C. elegans fertilization and encodes a sperm-specific transmembrane protein. Dev Biol *286*, 169-181.

67. Kadandale, P., Stewart-Michaelis, A., Gordon, S., Rubin, J., Klancer, R., Schweinsberg, P., Grant, B.D., and Singson, A. (2005). The egg surface LDL receptor repeat-containing proteins EGG-1 and EGG-2 are required for fertilization in Caenorhabditis elegans. Curr Biol *15*, 2222-2229.

68. Maruyama, R., Velarde, N.V., Klancer, R., Gordon, S., Kadandale, P., Parry, J.M., Hang, J.S., Rubin, J., Stewart-Michaelis, A., Schweinsberg, P., Grant, B.D., Piano, F., Sugimoto, A., and Singson, A. (2007). EGG-3 regulates cell-surface and cortex rearrangements during egg activation in Caenorhabditis elegans. Curr Biol *17*, 1555-1560.

69. Vacquier, V.D. (1998). Evolution of gamete recognition proteins. Science *281*, 1995-1998.

70. Alberts, B., Johnson, A., Lewis, J., Raff, M., Roberts, K., and Walter, P. (2002). The Molecular Mechanisms of Membrane Transport and the Maintenance of Compartmental Diversity. In Molecular Biology of the Cell, Fourth Edition. (New York: Garland Science).

71. Drenkard, E., Richter, B.G., Rozen, S., Stutius, L.M., Angell, N.A., Mindrinos, M., Cho, R.J., Oefner, P.J., Davis, R.W., and Ausubel, F.M. (2000). A simple procedure for the analysis of single nucleotide polymorphisms facilitates map-based cloning in Arabidopsis. Plant Physiol *124*, 1483-1492.

72. Jakubowski, J., and Kornfeld, K. (1999). A local, high-density, single-nucleotide polymorphism map used to clone Caenorhabditis elegans cdf-1. Genetics *153*, 743-752.

73. Marth, G.T., Korf, I., Yandell, M.D., Yeh, R.T., Gu, Z., Zakeri, H., Stitziel, N.O., Hillier, L., Kwok, P.Y., and Gish, W.R. (1999). A general approach to single-nucleotide polymorphism discovery. Nat Genet *23*, 452-456.

74. Zhao, L.P., Aragaki, C., Hsu, L., and Quiaoit, F. (1998). Mapping of complex traits by single-nucleotide polymorphisms. Am J Hum Genet *63*, 225-240.

75. Sarin, S., Prabhu, S., O'Meara, M.M., Pe'er, I., and Hobert, O. (2008). Caenorhabditis elegans mutant allele identification by whole-genome sequencing. Nat Methods *5*, 865-867.

76. Fay, D.S. (2008). Classical genetics goes high-tech. Nat Methods *5*, 863-864.

77. Livak, K.J. (1999). Allelic discrimination using fluorogenic probes and the 5' nuclease assay. Genet Anal *14*, 143-149.

78. Nairz, K., Stocker, H., Schindelholz, B., and Hafen, E. (2002). High-resolution SNP mapping by denaturing HPLC. Proc Natl Acad Sci U S A *99*, 10575-10580.

79. Wolford, J.K., Blunt, D., Ballecer, C., and Prochazka, M. (2000). High-throughput SNP detection by using DNA pooling and denaturing high performance liquid chromatography (DHPLC). Hum Genet *107*, 483-487.

80. Wicks, S.R., Yeh, R.T., Gish, W.R., Waterston, R.H., and Plasterk, R.H. (2001). Rapid gene mapping in Caenorhabditis elegans using a high density polymorphism map. Nat Genet *28*, 160-164.

81. Bruinsma, J.J., Schneider, D.L., Davis, D.E., and Kornfeld, K. (2008). Identification of mutations in Caenorhabditis elegans that cause resistance to high levels of dietary zinc and analysis using a genomewide map of single nucleotide polymorphisms scored by pyrosequencing. Genetics *179*, 811-828.

82. Davis, M.W., Hammarlund, M., Harrach, T., Hullett, P., Olsen, S., and Jorgensen, E.M. (2005). Rapid single nucleotide polymorphism mapping in C. elegans. BMC Genomics *6*, 118.

83. Swan, K.A., Curtis, D.E., McKusick, K.B., Voinov, A.V., Mapa, F.A., and Cancilla, M.R. (2002). High-throughput gene mapping in Caenorhabditis elegans. Genome Res *12*, 1100-1105.

84. Zipperlen, P., Nairz, K., Rimann, I., Basler, K., Hafen, E., Hengartner, M., and Hajnal, A. (2005). A universal method for automated gene mapping. Genome Biol *6*, R19.

85. Shakes, D.C., and Ward, S. (1989). Initiation of spermiogenesis in C. elegans: a pharmacological and genetic analysis. Dev Biol *134*, 189-200.

86. Geldziler, B., Chatterjee, I., and Singson, A. (2005). The genetic and molecular analysis of spe-19, a gene required for sperm activation in Caenorhabditis elegans. Dev Biol *283*, 424-436.

87. Gleason, E.J., Lindsey, W.C., Kroft, T.L., Singson, A.W., and L'Hernault S, W. (2006). spe-10 encodes a DHHC-CRD zinc-finger membrane protein required for endoplasmic reticulum/Golgi membrane morphogenesis during Caenorhabditis elegans spermatogenesis. Genetics *172*, 145-158.

88. Kadandale, P., and Singson, A. (2004). Oocyte production and sperm utilization patterns in semi-fertile strains of Caenorhabditis elegans. BMC Dev Biol *4*, 3.

89. L'Hernault, S.W., and Roberts, T.M. (1995). Cell biology of nematode sperm. Methods Cell Biol *48*, 273-301.

90. Bertrand, C.A., Laboisse, C., Hopfer, U., Bridges, R.J., and Frizzell, R.A. (2006). Methods for detecting internalized, FM 1-43 stained particles in epithelial cells and monolayers. Biophys J *91*, 3872-3883.

91. Washington, N.L., and Ward, S. (2006). FER-1 regulates Ca2+ -mediated membrane fusion during C. elegans spermatogenesis. J Cell Sci *119*, 2552-2562.

92. McCarter, J., Bartlett, B., Dang, T., and Schedl, T. (1999). On the control of oocyte meiotic maturation and ovulation in Caenorhabditis elegans. Dev Biol *205*, 111-128.

93. Miller, M.A., Nguyen, V.Q., Lee, M.H., Kosinski, M., Schedl, T., Caprioli, R.M., and Greenstein, D. (2001). A sperm cytoskeletal protein that signals oocyte meiotic maturation and ovulation. Science *291*, 2144-2147.

94. L'Hernault, S.W., and Arduengo, P.M. (1992). Mutation of a putative sperm membrane protein in Caenorhabditis elegans prevents sperm differentiation but not its associated meiotic divisions. J Cell Biol *119*, 55-68.

95. Machaca, K., and L'Hernault, S.W. (1997). The Caenorhabditis elegans spe-5 gene is required for morphogenesis of a sperm-specific organelle and is associated with an inherent cold-sensitive phenotype. Genetics *146*, 567-581.

96. Kadandale, P. Personal communication.